THE STUDY OF PEDESTRIAN LEVEL WIND AT MACGREGOR DOMITORY BUILDING

By

Teerawut (Lim) Wannaphahoon

SUBMITTED TO THE DEPARTMENT OF MECHANICAL ENGINEERING IN PARTIAL FULFILLMENT OF THE REQUIREMENT FOR THE DEGREE OF

BACHELOR OF SCIENCE IN MECHANICAL ENGINEERING
AT THE
MASSACHUSETTS INSTITUTE OF TECHNOLOGY

JUNE 2011

Signature of Author:_____

Teerawut Wannaphahoon
Department of Mechanical Engineering
May 6, 2011

Certified by:_____

Leslie K. Norford
Professor of Building Technology, MIT Department of Architecture
Thesis Supervisor

Accepted by: _____

John H. Lienhard V
Professor of Mechanical Engineering
Chairman, Undergraduate Thesis Committee

THE STUDY OF PEDESTRIAN LEVEL WIND AT MACGREGOR DOMITORY BUILDING

By

Teerawut (Lim) Wannaphahoon

Submitted to the Department of Mechanical Engineering
On May 6, 2011 in partial fulfillment of the
Requirements for the Degree of Bachelor of Science in
Mechanical Engineering

ABSTRACT

This study uses the Wright Brothers Wind Tunnel at MIT to study a 100:1 scaled model of the MacGregor dormitory building. The purposes are to quantify and analyze the effect of the presence of the building on pedestrian-level wind conditions, and to find the possible causes of an unusual strong wind condition around the corner of the building. Experiments were performed at 3 different angles of attack (0, 20, and 40 degrees) relative to the front of the model. Velocity measurements were taken at 16 different grid points, and a standard smoke experiment was done to visualize flow directions around the corner.

Velocity fields were plotted and normalized across the different grid points. Both magnitudes and directions of normalized values for different far-field wind speeds coincide very well. From the velocity fields, we observe a strong diverted wind across the building front along the pedestrian pathway. Moreover, we also find that, under certain conditions, the wind could accelerate up to 159% of the far field wind speed. The smoke experiment also demonstrates a streamline of airflow being diverted down to the pedestrian level.

Actual local wind speeds were obtained from a wind database, and were scaled using the normalized wind speed for each different grid point to obtain predicted wind speeds. Predicted wind speeds were categorized into different classes according to their magnitude. In the range that our study covers (0-40 degree angle of attack), the predicted wind is over an acceptable limit 7.87% of the time. Nonetheless, there is 38.81% of the time that the wind is strong enough to be felt on the body. These numbers are clearly not insignificant. However, further study needs to be done to extend the results of this study and propose and evaluate a solution to the problem.

Thesis Supervisor: Leslie K. Norford
Title: Professor of Building Technology, MIT Department of Architecture

TABLE OF CONTENTS

1. Introduction

It has been observed that the presence of buildings and human-made structures have a great impact, either accelerated or decelerated, on the wind speed as well as wind direction at pedestrian levels near the ground. There have been cases that a few tall buildings in the city acted as wind obstructions, which cause high wind at higher attitude to be diverted down to the pedestrian level, resulting in a strong wind speed that could be dangerous and uncomfortable for passersby. The famous cases in the Boston area are the Green Building at the Massachusetts Institute of Technology (MIT) and the John Hancock tower window incidents. In the Green Building case, the entrance to the building, which is located directly under the building in the tunnel-like opening of the first floor of the building, could not be opened under a high wind condition. There were speculation of the causes of the problem, and the MIT community wanted the problem to be addressed. In 1965, MIT Professor Joseph Bicknell conducted a series of wind tunnel tests at the MIT Wright Brothers Wind Tunnel using a scaled Green Building model to find the cause of the problem. In 1972, after a series of window incidents at the John Hancock building in Boston, a scaled wind tunnel test was also done on that building. The two cases made popular headlines in the news, making them two of the famous cases of MIT testing.

Apart from the stories of famous pedestrian level wind testing, it is now required by the Boston Redevelopment Authority (BRA), the Massachusetts Environmental Protection Agency (MEPA), and other regulatory agencies that the developers of new buildings verified the effect of the projects on the pedestrian level wind conditions around it (Durgin, 1989). The reason behind the requirement is to make sure that a pedestrian is safe to walk by the buildings as well as to prevent potential incidental damages that could be caused by such window falling accidents.

Located along the Cambridge side of the Charles River, MIT is vulnerable to high wind that could be accelerated due to an open water space. Apart from the Green Building case at MIT, which has already been addressed, students have also been experiencing high wind around the MacGregor dormitory building. The building, codename W61, is located at 450 Memorial Drive, Cambridge, MA, 02139. It is integrated in the array of dormitories along the pathway toward the west end of the campus. It consists of a tall tower together with a low-rise red-brick building surrounding it, forming a small court yard in the center; images are shown in Figures 1 and 2.

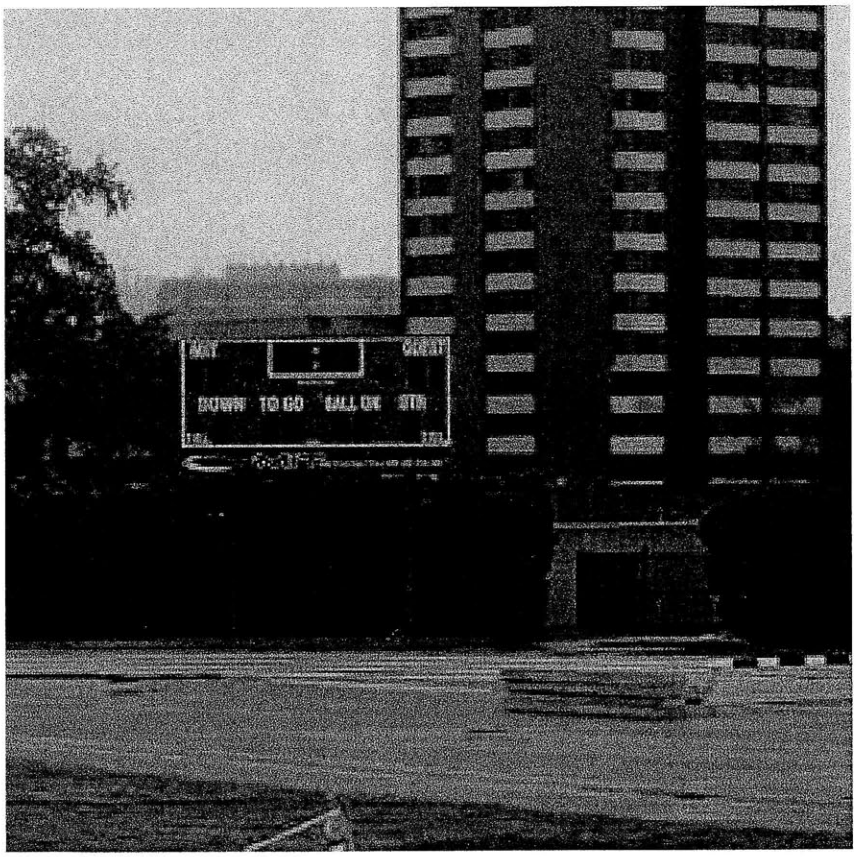

Figure 1: MacGregor from the North West View[1]

[1] The picture is obtained from the MIT facilities website

Figure 2: MacGregor from the North East View

The location of the strong wind experienced by students is along the pathway of Amherst Alley as seen from a pathway that a man is walking in Figure 2 and a spot in Figure 3. The pathway has a nickname among MIT students as "the MacGregor Wind Tunnel", referring to its usually strong wind characteristic. From my experience, the wind on the pathway is mostly blowing towards the east end of campus along the pathway (in the direction that the man in the picture is walking). Apart from occasional high wind gusts, the wind is steadily strong at this specific location. Nevertheless, there were times that the wind changes its direction to blow towards the west end of campus, and there were times that there was relatively no wind. However, for most of the time that there was no wind at this location, as long as I can remember, there was no wind overall around the Cambridge area on that day.

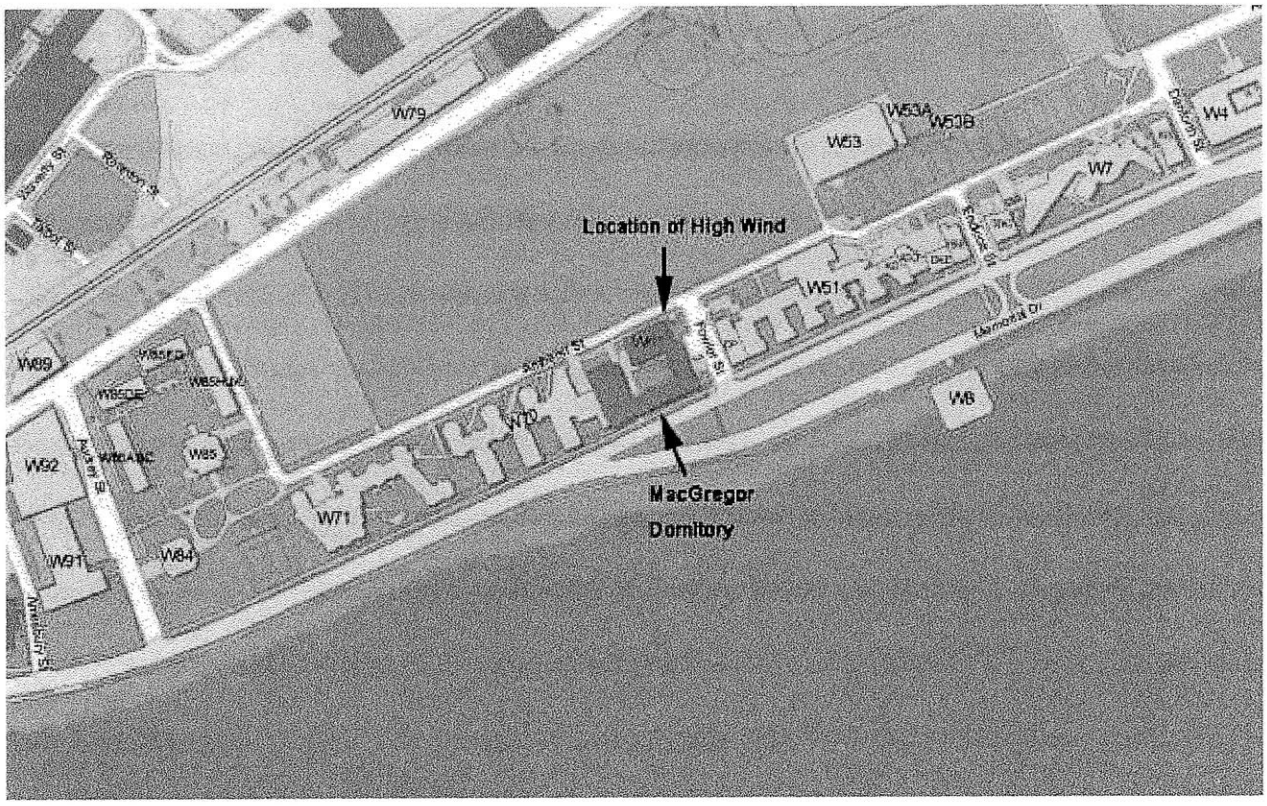

Figure 3: MacGregor Dormitory Map[2]

During my first year at MIT, I was not aware of the strong wind at MacGregor until winter had arrived. It was cold and it was windy. I was happened to wait for a Tech Shuttle (MIT transportation bus) at the bus stop in front of MacGregor. Then that I realized how uncomfortable it was for "the MacGregor Wind Tunnel" to be there – in the place where a lot of students had to walk pass by to other west-end dormitories or to wait for the shuttle bus to arrive. In fact, there was no properly sheltered bus stop, and students have to wait in the windy cold weather of Cambridge. I then was determined to find the cause of the problem and the reason why the wind was always strong at this particular location.

[2] Accessed from Google Map© on February 28, 2011

With my interest in finding out about the wind at MacGregor, during the Measurement and Instrumentation class at MIT (2.671), I did a term project [Go Forth and Measure project] on the comparison of wind speed at MacGregor (Wannaphahoon, 2009). In the project, I used an anemometer to measure the wind speed and compared the ones at MacGregor to those of other locations on campus. The wind speed at MacGregor was, unsurprisingly, statistically higher than that of the building nearby. I am interested in extending my Measurement and Instrumentation (2.671) project into a thesis in which I aim to perform a quantitative assessment of both the speed and direction of the flow structure of the building.

Aside from the fact that I want to extend my Go Forth and Measure Project into a thesis, I am also interested in a project that is related to the MIT Wright Brothers Wind Tunnel (WBWT) so that I can have a chance to experience the wind tunnel testing before I graduate from MIT. Moreover, I am interested in learning more about wind flow in modern urban areas as well as the methods that investigators are using to study the issues. Those interests fit very well with the goal of this project, and they motivate me to do the work. With my undergraduate experiences at MIT walking along the side of MacGregor countless times, I am also determined to find the cause to the problem so that in the future, MIT students would be able to enjoy life at MIT better by not having to experience the strong wind at the "MacGregor Wind Tunnel." All those are parts of the reasons that I would want to do this project.

As an undergraduate in the Energy Minor, I was planning that my thesis would involve such energy issues such as the possibility of redirecting the wind to power wind turbines to generate electricity. There are complications, I found out, about the ability to carefully simulate the effects of wind turbines in complex systems. Moreover, past researches have been done on actual measurement of wind at MacGregor to find the possibility of deploying wind turbines (Xu,

2011). Results have shown that, the wind at MacGregor is not as strong as those at the wind farm, and therefore, putting wind turbines there is not economically efficient. Therefore, I dropped the idea of analyzing the possibilities of the wind turbine system in my research, and focus on finding the cause of the problems instead.

2. Wind Tunnel Testing

Wind tunnel testing has been one of the focuses of aerodynamic research for a long time. Scientists and researchers have been using it to test wing design for aircraft, to measure drag on new designs of bikes, cars, and submarines, and etc. Moreover, it could also be used for low-level wind testing such as wind loads on buildings and pedestrian level wind condition around buildings.

MIT wind tunnel facility[3]

MIT has several wind tunnels on its campus, ranging from a student-made project to the massive Wright Brothers Wind Tunnel facility. The Wright Brothers Wind Tunnel has a long history with MIT. Many studies on various topics have been done at this facility. It is the source of many theses and a few breakthroughs in aerodynamic research.

The tunnel is a closed test-section wind tunnel with an approximately 7x10 foot elliptical cross section and a length of 15 feet. The size of the tunnel makes it possible to fit almost any instrument in it for testing. The tunnel could be pressurized and depressurized from 0.5 atm to 2 atm. However, due to complication of the pressurized test, this function is rarely in use. The picture of the inside of the tunnel is shown in Figure 4.

[3] The information in this section is from A Student's Guide to the Wright Brothers Wind Tunnel, accessed 03/30/11

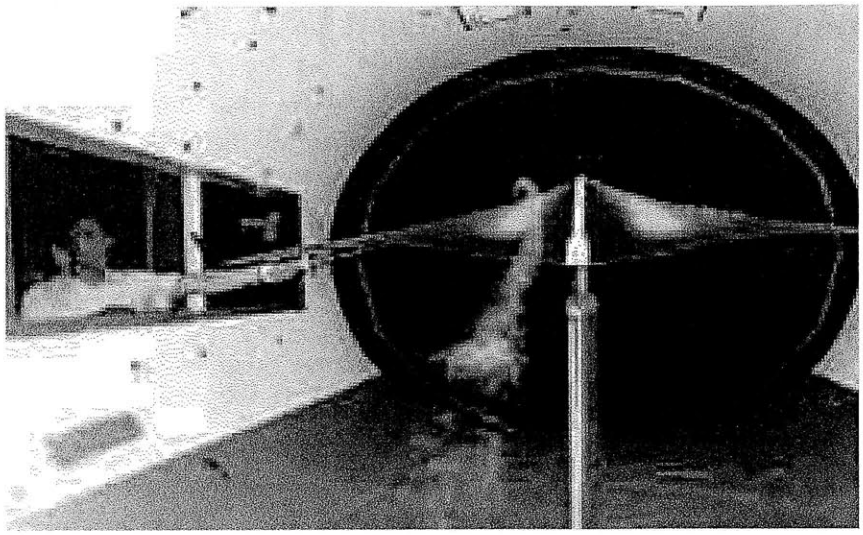

Figure 4: Inside the Wright Brothers Wind Tunnel

The wind inside the tunnel is generated by a 2000 HP fan that could generate the wind up to 150 mph (240 km/hr). The pitch setting of the fan blades control the airflow speed inside the tunnel. According to *A Student Guide to Wright Brother Wind Tunnel*, the standard deviation of wind speed around the range of testing (20-30mph) in the tunnel is less than 1% under no loading condition. With low variation of wind speed and wind direction on any cross section of the tunnel, for the propose of this study, I will assume that the wind is uniform in any cross section of the flow, and that it is equal to the speed that it is set.

Data Acquisitions in the Wind Tunnel Testing

There are two distinct sets of properties that researchers are trying to derive from the wind tunnel testing. First are the flow properties around the model. This includes mainly the values of dynamic pressure and static pressure, as well as velocity distribution at different points on and around the model. Flow properties will give useful information related to pressure loading, and velocity profiles are useful for structural engineers designing the buildings. Flow properties are

typically measured using pressure taps (for pressure) and an anemometer (for velocity). The second sets of properties are the flow directions of fluids around the model. The study of flow directions could be two dimensional, which in this case will study only the flow direction in the xy plane. This mainly suits for a typical structure that does not have a parabolic or hyperbolic profile that could generate an upward wind direction or studies that are not interested in the upward direction of wind (such as pedestrian level wind testing). Directional studies could also be three-dimensional, which are useful in the case of more complicated structures such as airplane wings. Directional studies could be derived from putting smoke into the air around the model to visualize the flow or putting tufts (small vertical pieces of materials) onto the body of model, and capture pictures of the visualized flow pattern.

- **Flow Properties Measurement**

Pressure is measured using pressure tap embedded within the structure. There are two types of pressure in the context of wind tunnel testing: dynamic pressure and static pressure. Dynamic pressure is the difference between the stagnation pressure and the static pressure. It could be used to derive velocity using Bernoulli's equation from the following equation. (Clancy, 1975).

$$q_{dynamic} = \frac{1}{2}\rho v^2 = q_{stagnation} - q_{static} \qquad (1)$$

As a result, some of the works obtain velocity distribution from (1) using the static pressure data.

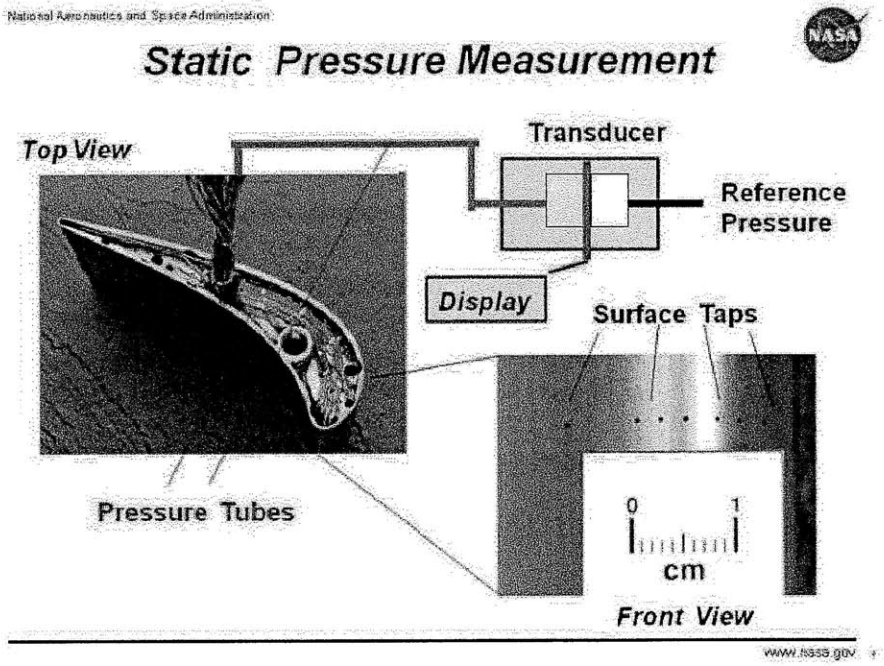

Figure 5: Pressure Taps[4]

Figure 5 shows an example of static pressure measurement in the test of an airplane wing. Pressure tubes are embedded in the model; surface taps (in the order of less than 1mm in diameter) are created to let an air flow to be in contact with pressure tubes in order to measure pressure. A typical wind tunnel model that is interested in finding the pressure distribution usually has tens or hundreds of pressure taps embedded on it.

[4] http://www.grc.nasa.gov/WWW/K-12/airplane/tunpsm.html (accessed April 17, 2011)

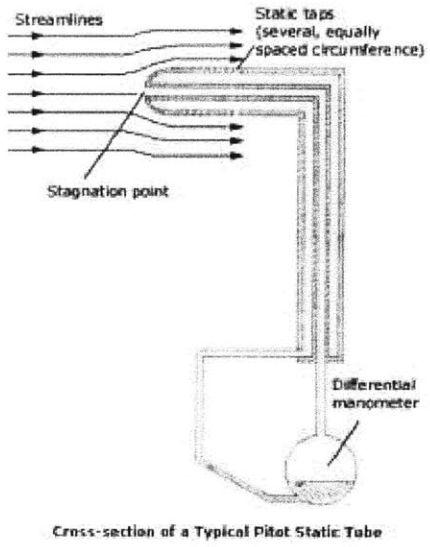

Figure 6: Pitot tube[5]

A pitot tube, as seen in Figure 6, is another measurement tool that measures both static and total pressure, which could be used to infer flow velocity. It is a separate piece of equipment that could be put on the floor of the model. The device is directional, and is subjected to different positioning of the equipment.

Apart from deriving velocity from dynamic pressure in equation (1), it is possible to measure velocity directly using an anemometer. Figure 7 shows an example of different types of anemometers.

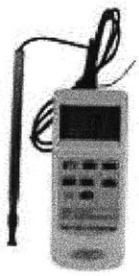

HWA4204HA Hot Wire Anemometer

Extech AN400 Rotating Cup Anemometer

[5] http://www.efunda.com/designstandards/sensors/pitot_tubes/pitot_tubes_theory.cfm (accessed April 17, 2011)

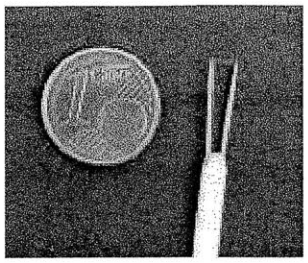

Tip of Hot-Wire Anemometer

Figure 7: Anemometer

A traditional cup anemometer uses drag on cups to estimate the wind speed based on the rotational velocity of the cup. The three-cup anemometer is an industry standard for measuring wind on local spots in buildings. A hot-wire anemometer, on the other hand, uses the rate of heat loss from the wire at the tip of the measurement tool to measure wind speed. The tip is usually kept at either constant current (CCA: Constant-Current Anemometer), or constant temperature (CTA:Constant-Temperature Anemometer).[6] The wind speed is measured from the amount of a parameter that is needed to keep the wire at each of the specified constant parameter. In contrast with cup anemometer, hot-wire anemometer is directional. The device usually has an opening at a certain direction in order to measure wind speed at that particular direction. A hot-wire anemometer has a small size and is sensitive to small changes in wind speed. These factors make hot-wire anemometer a good device for wind tunnel testing.

[6] http://www.efunda.com/designstandards/sensors/hot_wires/hot_wires_theory.cfm (accessed May 4, 2011)

- **Flow Direction Measurement**

Flow direction measurement in the wind tunnel is mainly done using the smoke and tufts techniques. However, there are other techniques, as shown in Table 1, that could be used as well to find other flow characteristics such as turbulent-laminar separation point or boundary layer condition in the flow.

Method	Flow Vis. On Model	Flow Vis. Off Model	Photos w/ Wind-on	Photos w/ Wind-Off	Effect on Data
Smoke	Yes	Yes	Yes	No	Small
Oil*	Yes	No	Yes	Yes	Small
China Clay	Yes	No	Yes	Yes	Small
Sublimation	Yes	No	Yes	Yes	Small
Minitufts	Yes	No	Yes	No	Very Small
Sewing Thread	Yes	No	Yes	No	Small
Tuft Probe	No	Yes	Yes	No	Variable

Table 1: Summary of different methods for flow visualization[7]

Smoke technique

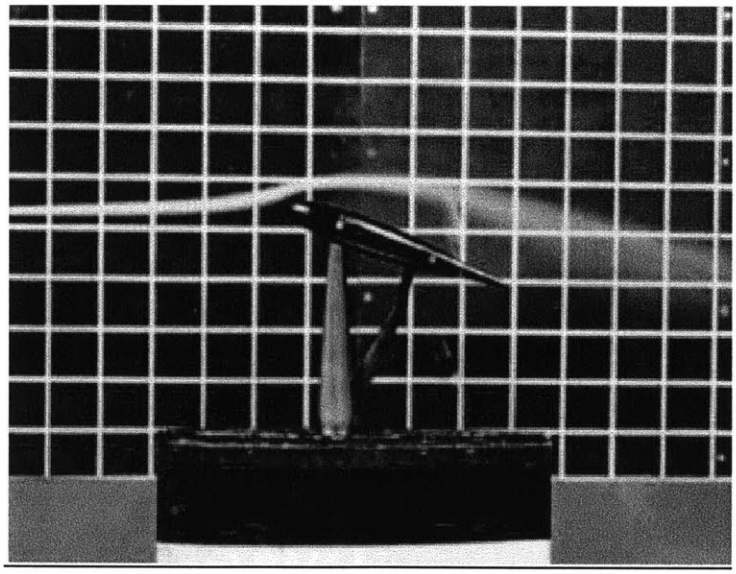

Figure 8: Smoke Flow Visualization Technique[6]

[7] http://www.uwal.org/contacts.htm (University of Washington Aeronautic Laboratory) (accessed April 17, 2011)

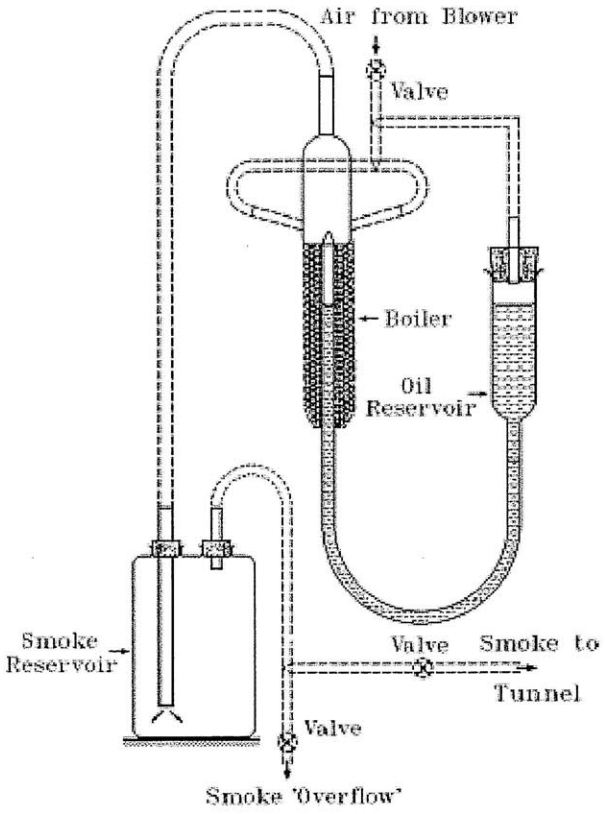

Figure 9: Smoke Flow Generator (Querin, 1993)

A smoke generator, as in Figure 9, is used to generate smoke at the upwind direction of the flow for visualization, as in Figure 8. The smoke method is easy to set up, and has little effect on the airflow properties inside the tunnel. An imaging device could be used to capture the smoke picture, and image-processing software could be used to analyze the flow data. The drawback of this technique, however, is the fact that the smoke has to be vented from the tunnel before it is filled completely with smoke. Moreover, oil residue could be left on the model where there is contact with the smoke. Pressure taps also need to be sealed in order to prevent malfunctioning.

Tufts Technique

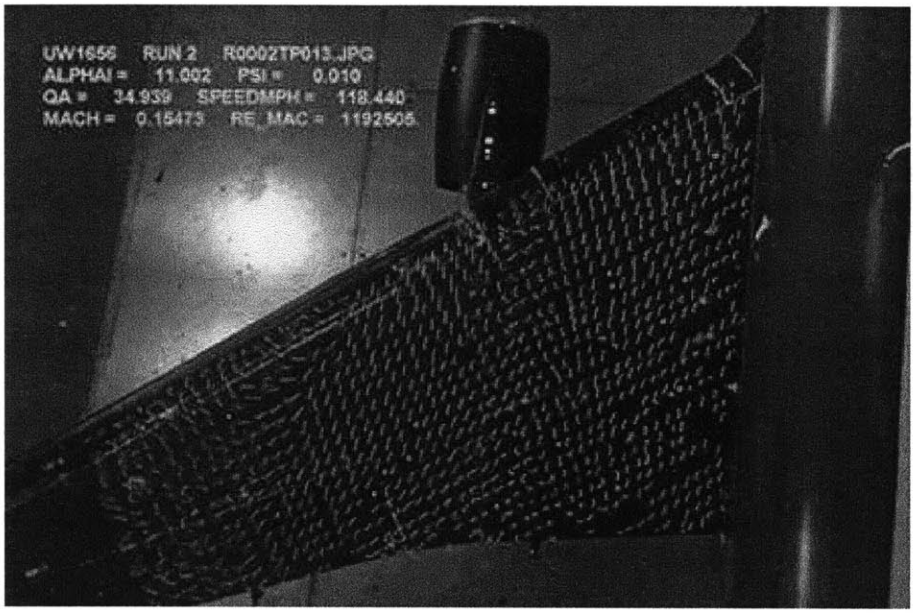

Figure 10: Tuft Flow Visualization Technique[8]

Another technique for flow visualization is the tuft technique, as seen in Figure 10. Small threaded tufts could be put on the surface of the model using either glue or tape. Fluorescent color could be put on the thread to enhance image contrast and image capturing quality. During the wind flow process, these small threads will align with the direction of the wind, and the flow direction could be analyzed from images taken from an imaging device. An advantage of this technique would be the fact that it allows wind direction to be measured across the surface at the same time. The threads themselves are also easy to set up, and have very little effect on the flow properties of the air around the model. The disadvantage, however, is the resolution that we can get from this technique. These threads are generally required to put at certain distance apart to ensure that they are not affecting each other.

[8] http://www.uwal.org/contacts.htm (University of Washington Aeronautic Laboratory) (accessed April 17, 2011)

Analyzing the Wind Tunnel Experiment

Non-Dimensional Analysis

Fluid behaves differently at different scales. In simulating what happens to a building at a larger scale by testing a miniature model in the wind tunnel, it is a standard to use non-dimensional analysis to present the results because the wind flow at a larger scale is subjected to different conditions. Non-dimensional analysis is an experimental tool that could be used to extend results from a smaller scale to a larger one.

Non-dimensional analysis is the tool that assumes the relationship between the physical properties of the world to be independent of units or dimension. In order to have a meaningful equation, both sides of the equations should have the same physical units. Non-dimensional analysis is trying to represent the equation in a unitless form, which could be used for scaling purposes in the case of scaling pattern.

Non-Dimensional Analysis for typical wind tunnel testing (Wright Brothers Wind Tunnel Student Guide)

Pressure and velocity from wind tunnel experiment should be non-dimensionalized to find the scaling factor to be able to extend it to a real physical condition.

Pressure could be non-dimensionalized as a pressure coefficient: $C_p = \frac{(P - P_{static})}{\frac{\rho v_{ref}^2}{2}}$.

Velocity could be non-dimensionalized using the free-flow velocity.

3. Previous Work: Wind Tunnel Tests on a model of the Earth Sciences Building [MIT Green Building] (Bicknell, 1965)

The Earth Sciences building at MIT has experienced a wind problem after the construction has been completed. The entrance door to the building could not be opened under certain wind conditions. In one of the incidences, one of the windows fell to the ground, and it was suspected that it was due to high pressure condition from the wind load.

Models of the Earth Sciences building as well surrounding buildings were built to be tested in the wind tunnel. Bicknell decided to use a scale of 96:1 to create the model. The reason for that scale size could not be found in the report, but I suspect that it is due to the constraint on the size of the wind tunnel. Pressure taps were installed throughout the model at various locations. The picture of the model is presented in Figure 11 below.

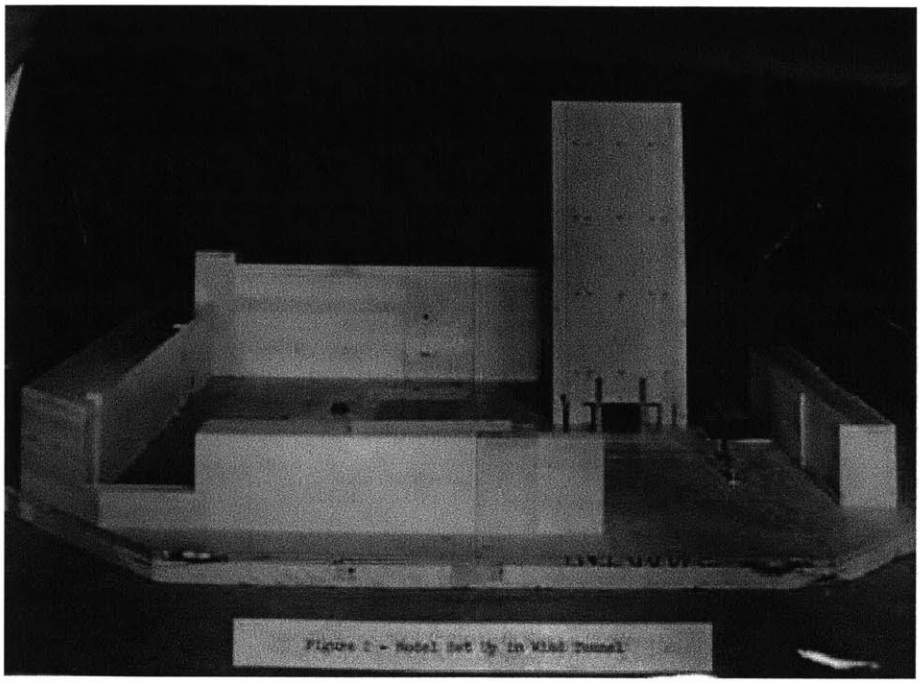

Figure 11: Earth Science Building Model

The model is made of wood and is mounted onto a plywood base to be able to rotate in the wind tunnel to simulate different wind condition and direction.

A vertical velocity gradient was created using non-uniform barriers to slow the stream at the lower level. The set up is designed to achieve the gradient value (α) of 0.3, and the wind to have the following distribution:

$$\frac{V}{V_1} = \left(\frac{Z}{Z_1}\right)^{\alpha}$$

The tests were to run at 60 and 65 mph across different attack angles. Pressure measurements were directly read off the tap and recorded by hand. The wind speed data was collected on top of the building using an anemometer. For near-ground velocity, direct velocity readings were made using a hot-wire anemometer.

Data was collected and non-dimensionalized using the pressure coefficient for pressure data and the far-field wind velocity (Wind Tunnel Velocity) for speed data. Results were presented. However, no direct recommendation was made about the solution to the high wind problem.

4. Wind Characteristic

Weibull Distribution (Jain, 2010)

There are several ways to represent wind data characteristics. The most accepted way to represent wind speed is the density distribution called Weibull:

$$pd(v) = \frac{k}{A} * \left(\frac{v}{A}\right)^{k-1} * e^{-\left(\frac{v}{A}\right)^{k}}, v > 0 \qquad (2)$$

Where v is the wind speed, k is the shape factor, and A is the scale factor of Weibull. By changing the shape factor, k, and the scale factor, A, one could fit the Weibull model to most the wind conditions. In the case of k=1, the distribution becomes an exponential distribution. For k=2, the distribution becomes a Rayleigh distribution. For k>3, the distribution approaches a Gaussian distribution. Values of k between those integers bridge the transition between each distribution.

As k increases, the height of the curve increases. This implies that the tail will become narrower, which means that the probability for high wind is less. In general, if two wind distributions have the same average wind speed, the one with the higher k will have lower probabilities of high wind speed and consequently lower energy. An example of a Weibull distribution is shown in Figure 12.

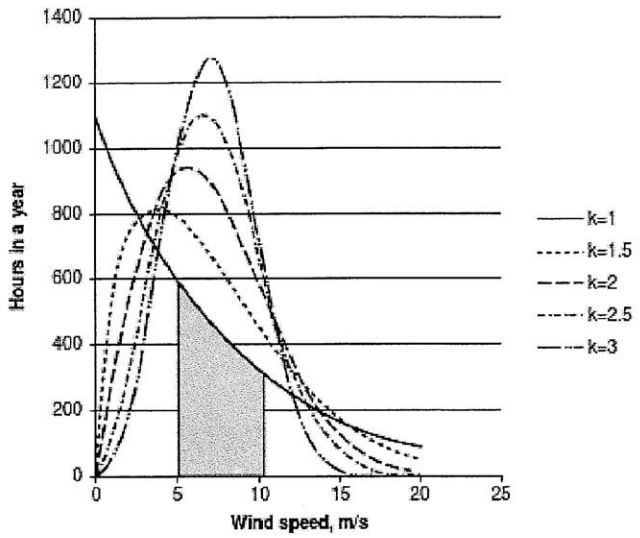

Figure 12: Weibull distribution (Jain, 2010)

Wind Classes (Jain, 2010)

The strength of the wind at different locations is based on the power density of wind at the location at the height of 50 meters. The distribution is shown in Figure 13. Different classes of wind are used, for example, to find a location to put wind turbines to harvest wind energy. It can also be used to differentiate different wind loading conditions that buildings are likely to face in certain areas.

	10 m		50 m		
Wind Class	Wind Class Name	Power Density, W/m^2	Average Wind Speed, m/s	Power Density, W/m^2	Average Wind Speed, m/s
1	Poor	0–100	0–4.4	0–200	0–5.6
2	Marginal	100–150	4.4–5.1	200–300	5.6–6.4
3	Fair	150–200	5.1–5.6	300–400	6.4–7.0
4	Good	200–250	5.6–6.0	400–500	7.0–7.5
5	Excellent	250–300	6.0–6.4	500–600	7.5–8.0
6	Outstanding	300–400	6.4–7.0	600–800	8.0–8.8
7	Superb	400–1000	7.0–9.4	800–2000	8.8–11.9

* Wind speed ranges and power density are at specific heights.

Figure 13: Wind Classes (Jain, 2010)

Wind Shear (vertical velocity distribution)

Due to the no-slip condition along the surface, the wind speed near the surface is close to zero, and the distribution of variation of wind speed along height is best described by the following equation:

$$\frac{v_2}{v_1} = \left(\frac{h2}{h1}\right)^y \qquad (3)$$

In some realistic conditions, equation (3) is modified to have the roughness factors in it as follows:

$$\frac{v_2}{v_1} = \frac{\ln\left(\frac{h_2}{z_0}\right)}{\ln\left(\frac{h_1}{z_0}\right)} \qquad (4)$$

$$y = \ln\left(\frac{\ln\left(\frac{h_2}{z_0}\right)}{\ln\left(\frac{h_1}{z_0}\right)}\right) / \ln\left(\frac{h_2}{h_1}\right) \qquad (5)$$

Where z_0 is the roughness of the surface, and y is the shear of the distribution. With a known velocity point v, and a roughness value z_0, one could extrapolate to find other velocity point at different height. The effect of shear on the velocity distribution is shown in the figure below:

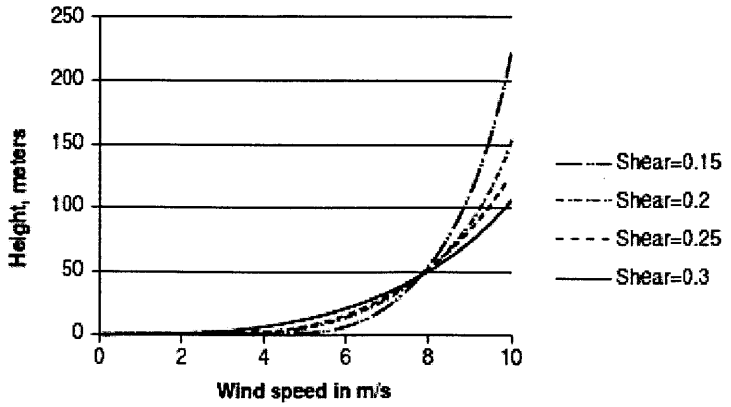

Figure 14: Effects of Wind Shear on Velocity Distribution (Jain, 2010)

Table 2 also shows different shear values depending on different structural conditions. It is observed that the roughness value increases as the system gets more complex. The lowest reference roughness value could be found on an open sea, where the wind is observed to be generally strong.

Description	Roughness Class	Roughness Length, m	Shear
Open sea	0	0.0001–0.003	0.08
Open terrain with a smooth surface, like concrete runway, mowed grass	0.5	0.0024	0.11
Open agricultural area without fences and hedgerows and very scattered buildings. Only softly rounded hills	1	0.03	0.15
Agricultural land with some houses and 8-m-tall sheltering hedgerows with a distance of approx. 1250 m	1.5	0.055	0.17
Agricultural land with some houses and 8-m-tall sheltering hedgerows with a distance of approx. 500 m	2	0.1	0.19
Agricultural land with many houses, shrubs and plants, or 8-m tall sheltering hedgerows with a distance of approx. 250 m	2.5	0.2	0.21
Villages, small towns, agricultural land with many or tall sheltering hedgerows, forests, and very rough and uneven terrain	3	0.4	0.25
Larger cities with tall buildings	3.5	0.8	0.31
Very large cities with tall buildings and skyscrapers	4	1.6	0.39

Source: Nielsen, Per. WindPRO 2.5 Users Guide. EMD International, Aalborg, Denmark, 2006.

Table 2: Different Shear Values (Jain, 2010)

5. Experimental Section: MacGregor Wind Tunnel Test

Model Design and Construction

Model design and construction play an important role in the wind tunnel research and testing. Ideally, we would like the model to have the same characteristics as the actual building. We would like the model to have the same length-scale and details as the actual building. Moreover, we would also like to generate the wind with similar boundary condition, turbulence level, and velocity distribution as the typical wind in a typical day of a year. However, due to size limitation, the model that could go into the wind tunnel could not be as large as the actual building. The bigger the model is; however, the better and more accurate representation of the actual situation since the Reynolds number,$Re = \rho vL/\mu$, depends on the characteristic length scale L. The bigger L is, the closer the model Reynolds number to the actual Reynolds number, and the more we can assure that the flow in the model and the actual flow are in the same regime (eg. laminar, transition, or turbulent). Air speed in the tunnel can also be increased to partially compensate for the smaller length scale. Greater details on the model represent a more realistic view of the building; nevertheless, it makes it much harder to construct. It is safe to assume that materials that are used to build the model also have an important factor on the surface roughness, which also has a direct effect on the near surface boundary layer.

Scale of the model

The scale I chose to work with my model is 100:1. This value is chosen primarily from the value of 96:1 chosen by MIT Professor Bicknell in his work on the Green Building (Bicknell, J., Shaw, A., 1965). This value represents the largest model scale that could be put into the Wright

Brothers Wind Tunnel facility at MIT. This, however, infers a factor of 100 reductions in Reynolds number, assuming we use a similar magnitude of wind in the tunnel. As a result, we need to verify whether the Reynolds number that governs the scale model and the one that govern the actual building fall in the similar regime.

Boundary layer Reynolds number calculation

In the actual atmosphere, the wind is highly turbulent around such complex structures as buildings. Using an average velocity of 3.74m/s (Kalmikov et al. experimental average at 20m from ground on MIT site, 2010), the length scale of 32m (the actual length of the side wall of the building where there suspects to be high winds), and the kinematic viscosity of air at 300K at $15.68 * 10^{-6} m^2/s$. The Reynolds number could be calculated as:

$$Re = \frac{VL}{\upsilon} = 7.63 * 10^6$$

This Reynolds number exceeds the transition value of $5 * 10^5$ for a typical boundary layer, and as a result, the last part of the boundary layer in the actual building is likely to be turbulent. At the wind tunnel speed of 30mph (13.41m/s), the Reynolds number of the model could be calculated using the same kinematic viscosity to be Re = 270,000, which is still less than the transition cut off for the turbulent regime. This implies that our test conditions are mostly in the laminar regime. In some of the modern wind tunnels, there are equipments that are used to generate turbulent-like condition in the tunnels, but unfortunately, the facility that we have at MIT does not have one. The study of laminar regime in the tunnel, however, will give us the basic picture, if not completed, of what the air flow is like in the actual building.

Details on the model

Windows and minor details of the buildings are removed. Moreover, details on the side that is not facing the wind are greatly reduced than the side that is facing the wind. The main structure, however, is kept the same. Simplifying the model does not reduce the general effect of the building on wind flow, but it will help save a lot of time that has to be spent building the model.

Materials

The material I use to make a model is plywood. The model is attached to the base that is made from an MDF material. Plywood is chosen because it is relatively smooth. It is also easy to manufacture, cheap, and easy to find. Bicknell and several subsequent researchers in pedestrian wind level testing also used plywood for the model in his Green Building and other studies. MDF has a relatively low roughness level, which is good for the base of the wind tunnel model.

Model Construction

Solidworks is used for the designing purposes. Please see Appendix 1 for pictures of the design and model construction.

The model was built in the MIT hobby shop using several wood processing machines. The final base size of the model is 5'x6'. The model has a height of 18.60" at the top of the tower.

6. Method of Testing and Measurement

Equipment

The hot-wire anemometer that I used for measuring the wind velocity is TSI model number 8345/8346 as shown in Figure 15.

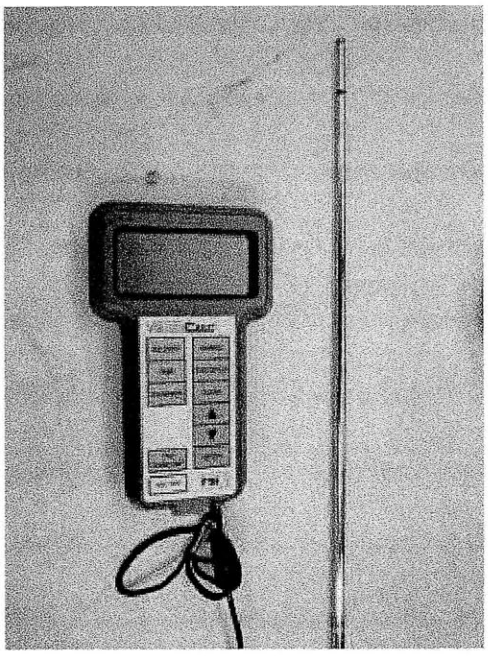

Figure 15: Hot-wire anemometer used in the experiment

This hot-wire anemometer has a telescoping rod that could be used to extend down to the base level to measure velocity without much of disruption. The accuracy of the reading is 3% of the reading or a maximum of ± 0.015 m/s, well below the range that we are interested in. Therefore, the reading is treated as fairly accurate. Measurements were done by hand with me using the instrument to measure velocity at different grid points. The read out was set to display an average over an interval of 5 seconds for better accuracy.

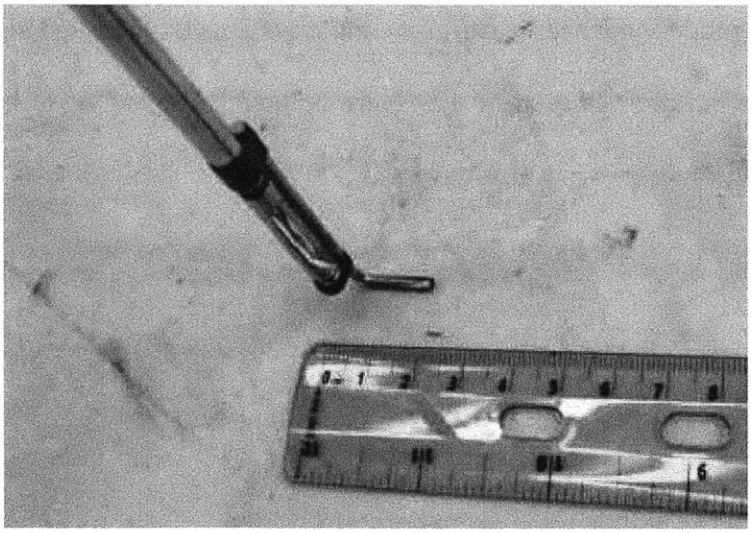

Figure 16: Tip of hot-wire anemometer

The tip of the hot-wire anemometer was modified to be able to tell the direction of wind speed that it was measuring by attaching a hex key to the end of the tip along hole opening (see Figure 16). The height that the tip was touching the ground from the actual sensor (the wire) was set to be 2cm, which represents the actual height of 2m of a human body. In order to quantify each component of wind speed, we measured each of the velocity components, Vx and Vy, at the height of 2cm above the ground level.

Wind Tunnel Matrix

A wind tunnel matrix, shown in Table 3, represents a set of conditions (angle, wind speed) for which I planned to test the model.

Test Matrix			
Velocity/Angle of Attacks (degrees)			
20mph	0	20	40
25mph	0	20	40
30mph	0	20	40

Table 3: Wind Tunnel Test Matrix

I planned to test the model under three different angles of attack: 0, 20 and 40 degrees relative to the north axis of the building as seen in the figure below. These angles of attack correspond to the main direction of wind speed (Kalmikov et al., 2010) that the building is experiencing. They are also the main angles that are likely to cause the high wind speed at the corner of the building.

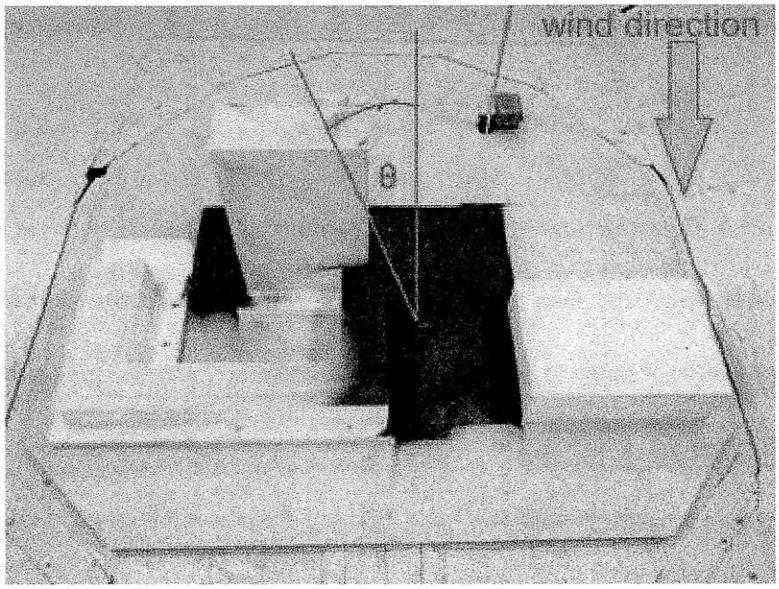

Figure 17: Model Angle of Attack

I planned to run the test at three different speeds, namely 20mph, 25mph, and 30mph for each of the angle of attack. These speeds are limited by the danger of the speed to the presence of human (I must be in the tunnel to take the measurements). Even though these speeds are lower than what Bicknell used in his studies (60mph), it still proposes the similar range of Reynolds number with that of the faster speed. In order to compensate for the presence of me inside the tunnel, the tunnel operator continually adjusted the pitch of the fan blade to keep the wind speed nearly constant. Portions of the model were painted black to aid the visualization processes during the smoke experiments.

Grid Point Location

Data were collected at 16 different grid points of interest. Fourteen grid points are used to capture the flow behavior around the corner of the building. The remaining two grid points are put in the channel between the two buildings to measure the Venturi effect of wind between the buildings. The locations of the grids are shown in the figure below.

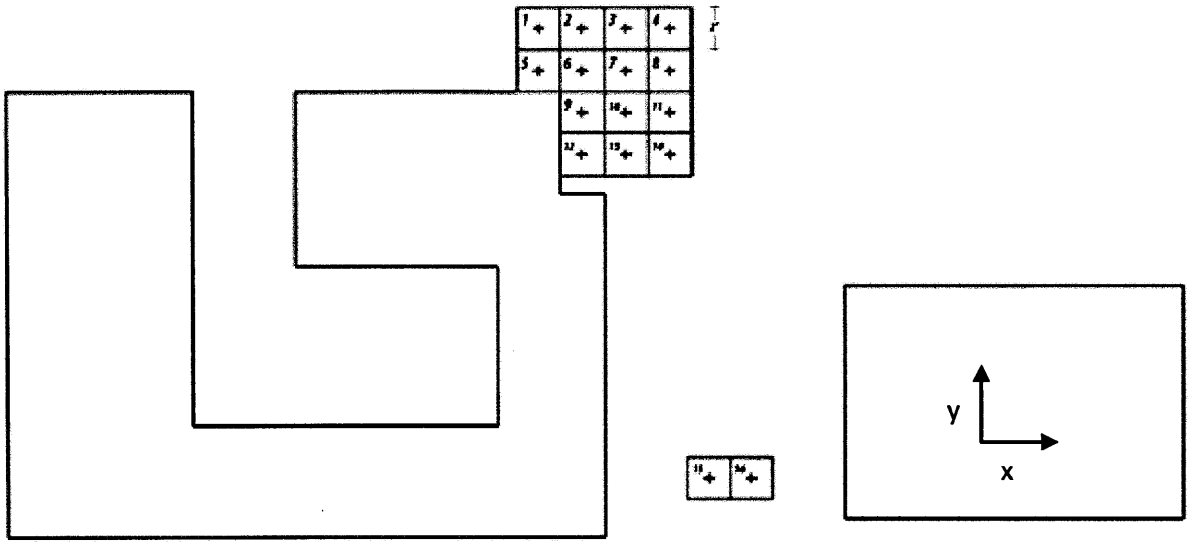

Figure 18a: Grid Points of Interest

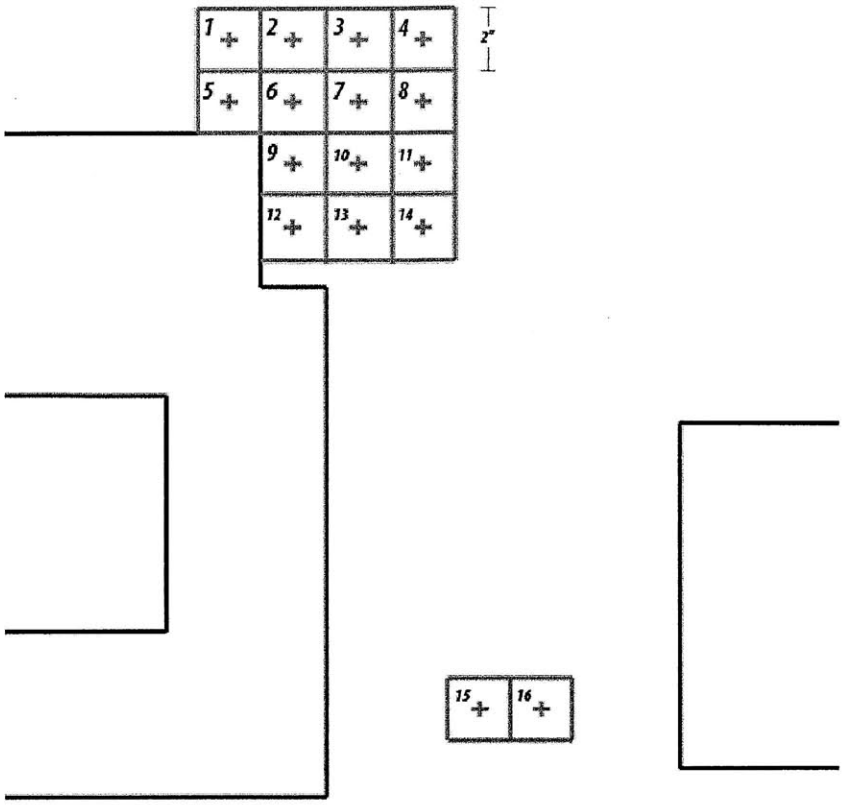

Figure 18b: Grid Points of Interest

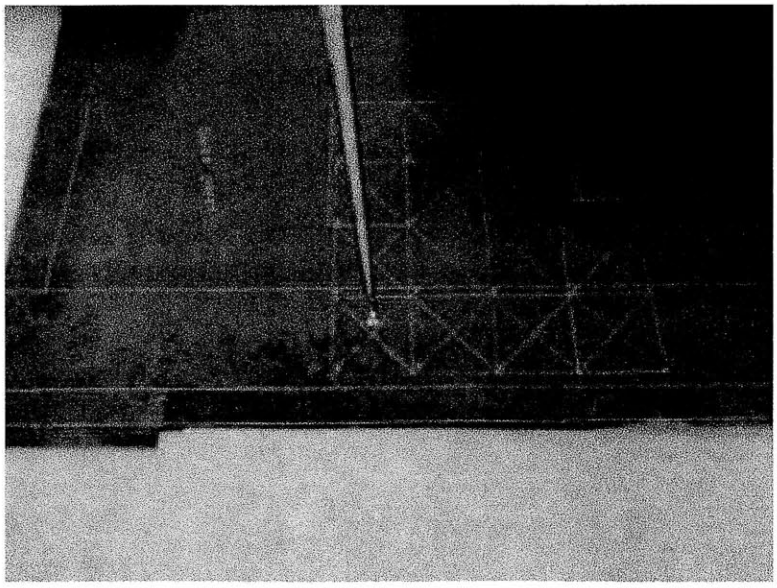

Figure 18c: Grid Points of Interest and Measurement

Velocity Measurement

Measurements of velocity were done using TSI8345/8346 hot-wire anemometer. For each of the grid points, two measurements of velocity were done along the x and the y axes to measure each components of the velocity vector. The instrument was lowered down to the height of 2 centimeters above the floor, equivalent to the height of 2 meters in the actual setting. The tip of the measurement tool has a pin point that could tell the direction in which the tool was measuring. These measurements were done physically by human, and the readings were collected manually.

Smoke Directional Velocity Measurement

Figure 19: Smoke Directional Measurement

A smoke generator created smoke to visualize a streamline of air as it being passed through the structures similar to Figure 19. A smoke tube was controlled by hand, and was put into a desired

location. Video was captured during the entire experiment, and images for analysis were derived from the video.

The smoke experiments were done at the wind speed of 30mph, and at the angle of attack of 0 degree.

Shear Layer

In this experiment, artificial shear layer was not created; therefore, there was not a large boundary layer that could be described by equation (3). In the actual building, however, the wind has accelerated through the wide open field in front of the building with few obstacles. With a low shear value of an open area, the condition could be said to be similar, if not the same, to the wind tunnel condition with no artificial shear layer. Therefore, the wind tunnel with no artificial shear could be used to demonstrate results, if not complete, of the pedestrian level wind experiments.

7. Results

Wind Velocity Results

Numerical results are presented in Appendix 2 and Appendix 3 of the paper. Actual velocity values are presented in Appendix 2, and normalized values are presented in Appendix 3. Normalized values are created by dividing actual values by the far-field velocity corresponding to each of the experiments.

Figures 20 and 21 present actual and normalized velocity fields at different angles of attack. Velocity fields were created in Matlab©. Each of the actual velocity values is reduced by a factor of 10 in order to fit in the vector field box in the vector field plot function. Since it is already scaled, the normalized velocity field plot is not subjected to any additional scaling in Matlab©.

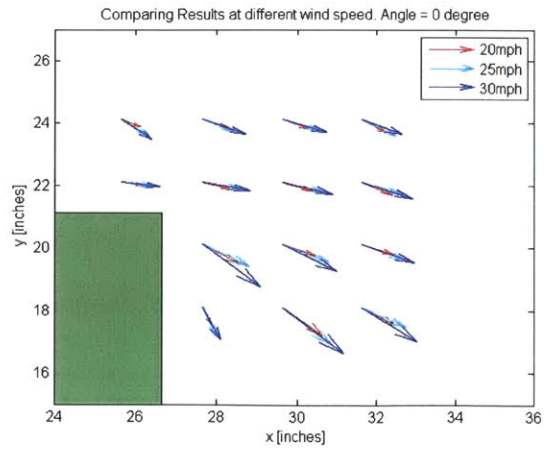

(1)

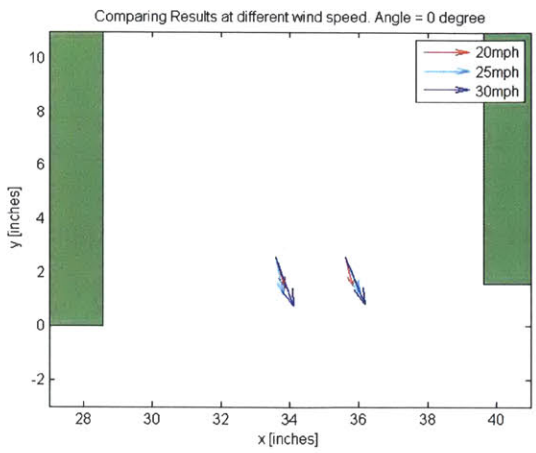

(2)

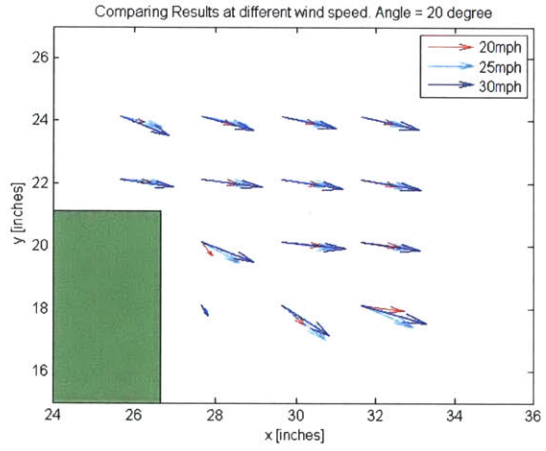

(3)

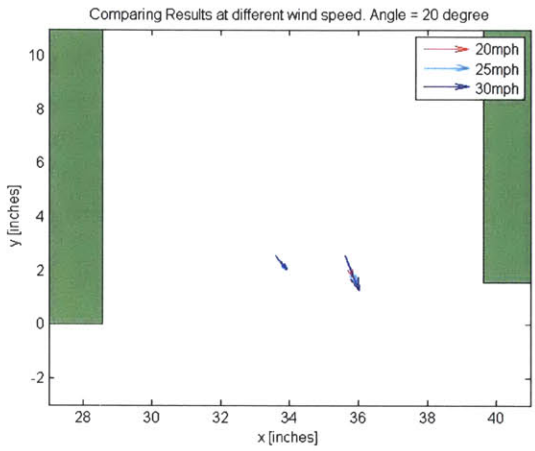

(4)

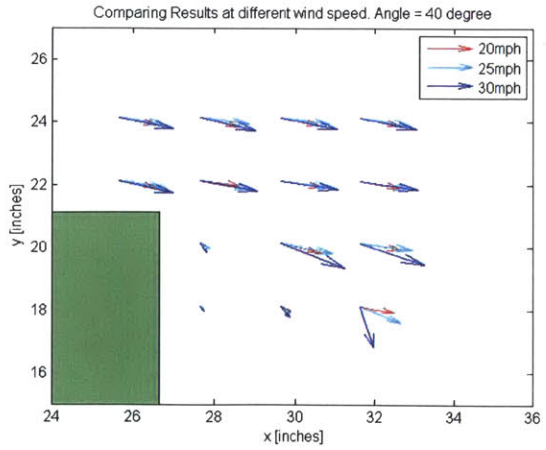

(5)

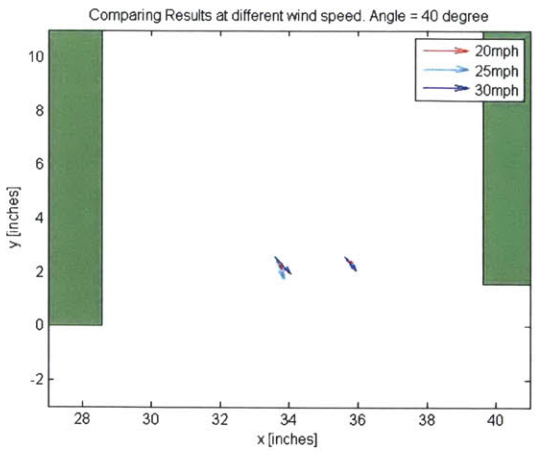

(6)

Figure 20: Actual Velocity Field

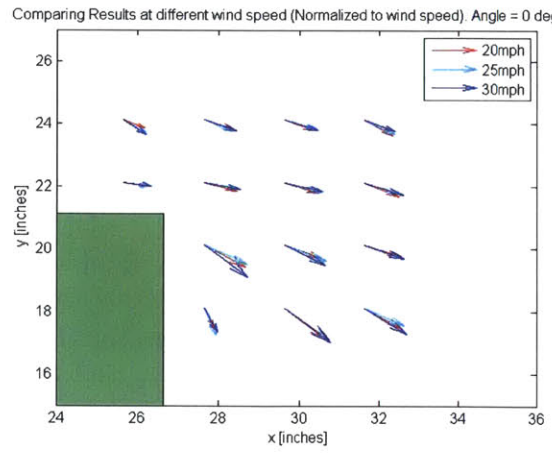

(1)

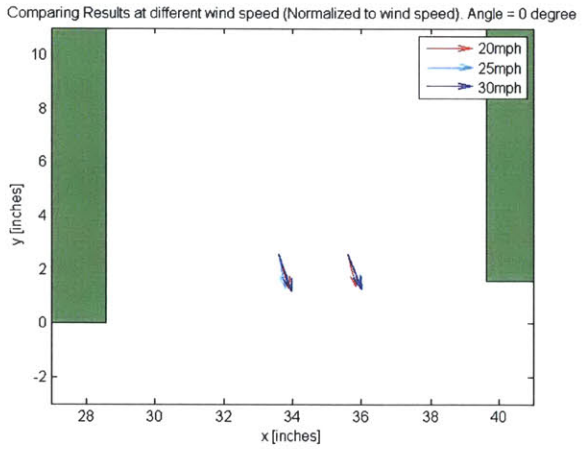

(2)

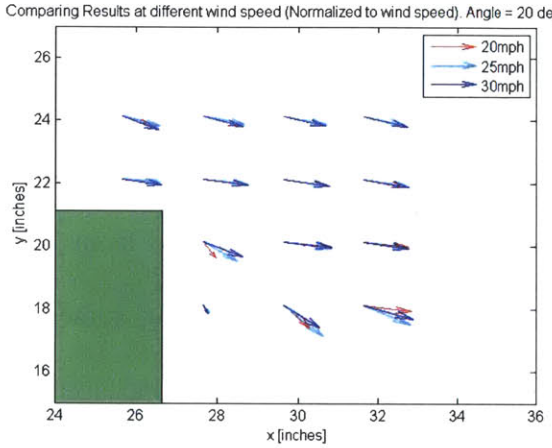

(3)

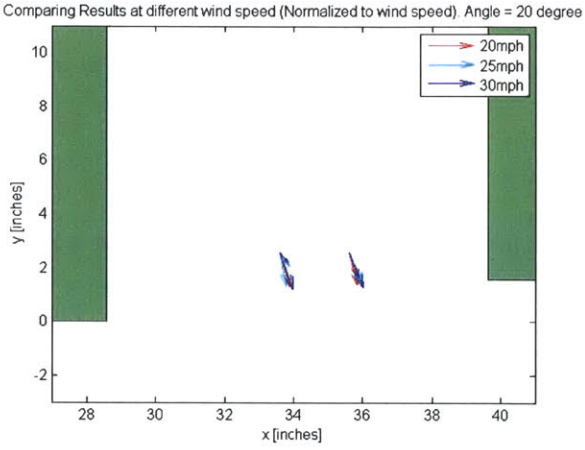

(4)

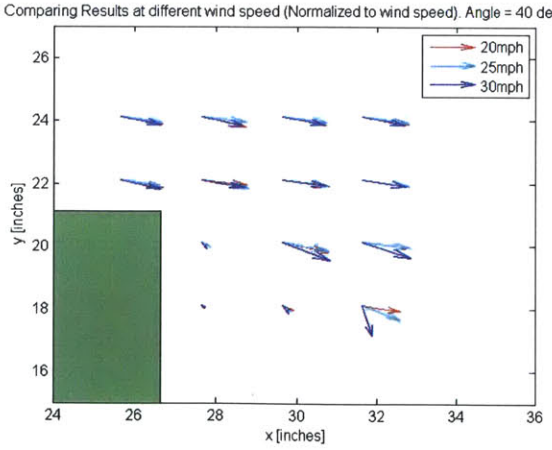

(5)

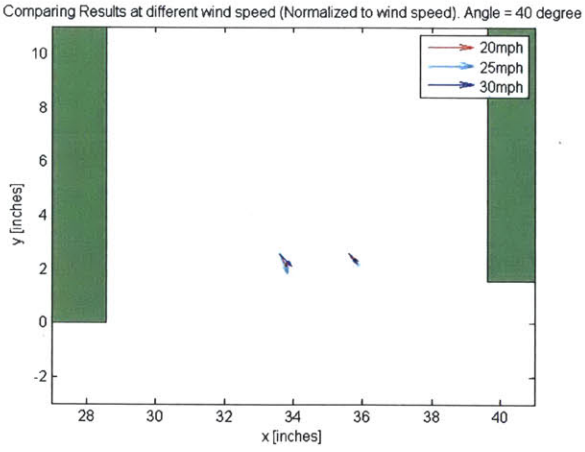

(6)

Figure 21: Normalized Velocity Field

The velocity fields indicate that the structure of the building has induced a strong wind in the x-direction (parallel to the pathway). We do not observe, however, the point of separation, where the flow is turning back to the y-direction in order to pass through the channel.

Normalized velocity fields also show an interesting result. Normalized velocity fields greatly coincide in both the magnitude and direction for each different far field wind speed for GRID 1-8. Suspected turbulent spots in the shadow of the building (GRID 9-14) shows non-uniform velocity data for different wind speed as we could expect from the turbulent condition. This uniformity in GRID1-8 gives us confidence to use the normalized velocity fields at those grid locations to scale up the actual wind flow, which we will present the result later in the discussion section.

In terms of the magnitude of wind at each of the grid locations, the data varied from 29% to 159% of the far-field wind velocity. This indicates that we are currently seeing some of the accelerated wind condition around the building. Table 4 shows the magnitudes of measured wind tunnel experiment as the percentage of corresponding far-field velocity. The magnitude of at each point is assumed to be the square root of the sum of the squares of velocity in the x and y directions.

Tunnel Speed (mph)	**20**	**20**	**20**	**25**	**25**	**25**	**30**	**30**	**30**
Grid/Angle	0	20	40	0	20	40	0	20	40
1	59%	74%	107%	75%	96%	103%	73%	101%	104%
2	78%	100%	116%	75%	106%	110%	87%	103%	107%
3	77%	104%	114%	86%	109%	112%	88%	106%	109%
4	86%	103%	119%	89%	102%	116%	84%	114%	109%
5	62%	91%	109%	67%	95%	103%	71%	99%	105%
6	86%	110%	115%	87%	109%	118%	90%	113%	109%
7	90%	115%	119%	95%	112%	116%	98%	116%	109%
8	97%	109%	118%	96%	112%	116%	103%	115%	112%

9	124%	60%	21%	121%	102%	28%	147%	108%	25%
10	100%	121%	118%	114%	120%	121%	118%	120%	133%
11	97%	115%	120%	102%	108%	120%	108%	113%	131%
12	65%	26%	13%	90%	28%	12%	85%	29%	13%
13	150%	98%	33%	151%	140%	30%	159%	113%	31%
14	115%	123%	99%	114%	132%	105%	133%	131%	100%
15	131%	50%	56%	125%	57%	77%	140%	45%	57%
16	122%	91%	39%	125%	103%	52%	136%	102%	46%
Max	150%	123%	120%	151%	140%	121%	159%	131%	133%

Table 4: Magnitude of Wind Speed at Different Grid Points

Looking at GRID 5-8, which are along the actual pedestrian pathway, we can see that the magnitude of wind increases as the angle of attack increases. The majority of these velocity components are also in the x direction, forcing the wind directly on pedestrians. At the angle of attack of 40 degree, magnitudes of the wind are all greater than 100% for all GRID1-8. This indicates that we have found that the wind has accelerated along the path of MacGregor. The reason for this acceleration is still not known for certain. However, the degree of acceleration is not as high as expected, ranging from 100% to 120% of the far-field wind speed.

Smoke Experiment Results

(1)

(2)

(3)

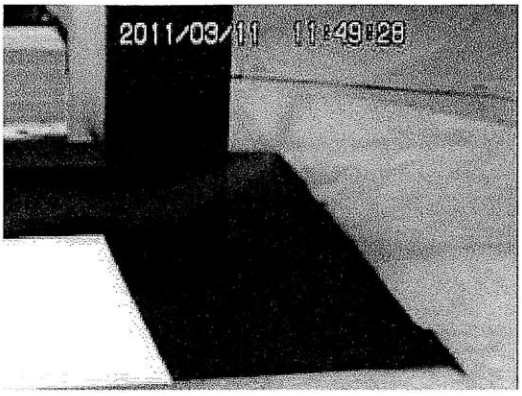

(4)

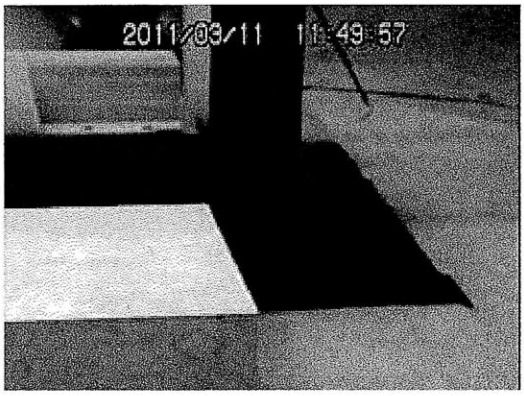

(5)

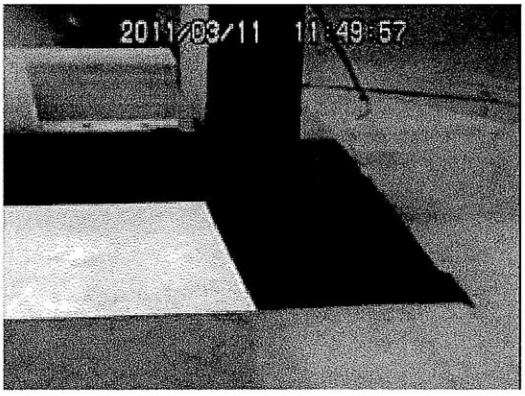

(6)

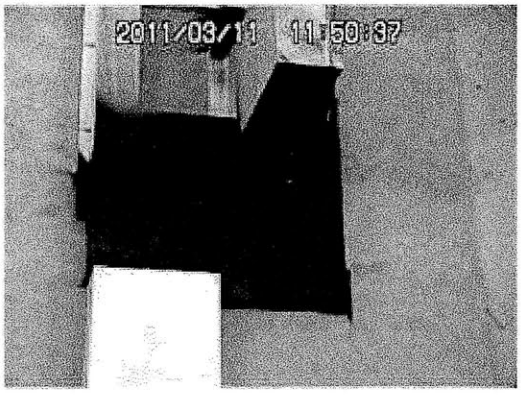

(7)

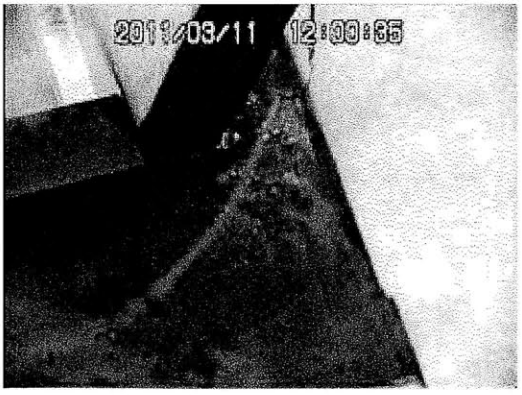

(8)

Figure 22: Smoke Experiment Pictures

The smoke experiment was done for the model setting up at zero degree (perpendicular to the wind), with the wind in the tunnel set up at 30mph.

Subfigures (1) and (2) of Figure 22 show the wind direction near the edge of the building. We can see that it forms a curved streamline that follows the edge of the building, creating the strong horizontal velocity component (Vx).

Subfigures (3) – (6) shows another interesting result. They demonstrate that the wind is diverted down to the ground level due the geometry of the building. In particular, we can see that the streamline of the wind at moderate height was diverted down to ground level around the corner.

Powder Experiment

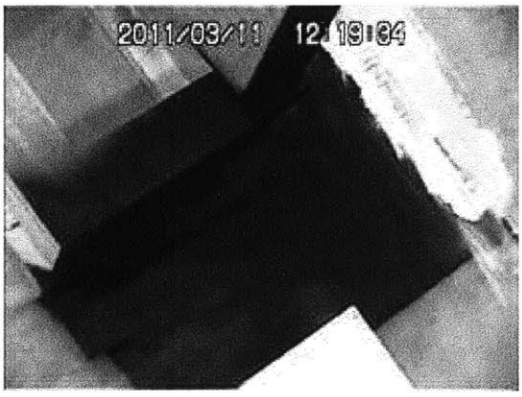

(1)

(2)

(3) (4)

Figure 23: Powder Experiment Pictures

The powder method was tried by putting a small amount of powder in front of the building. The wind tunnel was turned on to the speed of 60mph to generate the flow path. The ground level streamline was observed using the trace of powder shown in subfigure (4) of Figure 23.

8. Discussion

A.D. Penwarden (1973) has written a paper indicating effects of different wind speed on people.

Table 5 summarizes his results:

Class	Speed (m/s)	Effects
1	0-1.5	Calm, no noticeable wind
2	1.6-3.3	Wind felt on face
3	3.4-5.4	Wind extends light flag. Hair is disturbed. Clothing flaps.
4	5.5-7.9	Raises dust, dry soil, and loose paper. Hair disarranged.
5	8.0-10.7	Force of wind felt on body. Drifting snow becomes air-borne. Limit of agreeable wind on land.
6	10.8-13.8	Umbrellas used with difficulty. Hair blown straight. Difficult to walk steadily. Wind noise on ears unpleasant. Windborne snow above heat height (blizzard).
7	13.9-17.1	Inconvenience felt when walking.
8	17.2-20.7	Generally impedes progress. Great difficulty with balance in gusts.
9	20.8-24.4	People blown over by gusts.

Table 5: Effects of Wind Speed on People (Penwarden, 1973)

In order to quantify the result of my experiment, I will use absolute values of normalized wind speed at different grid points as a scaling factor for the data on actual wind speed in order to obtain a predicted wind speed at different grid points as a result of the incoming wind. It will allow us to quantify, to the first order, the seriousness of the high wind condition at MacGregor by making a distribution of each of the wind classes that different grid points have over the course of a typical year.

Wind Speed Data

The wind data that I will be using is from the roof of the MIT green building. I think that this database is the best to represent the wind condition around the MacGregor building and Briggs

Field due to its proximity to the locations, rather than a faraway traditional location like the wind database from Logan Airport.

Wind speed data is collected from www.wunderground.com on April 14, 2011 using a user-generated Python data collection program. The code for the station is KMACAMBR9, which refers to the roof of the green building on the MIT campus. The database comprises the wind data that was collected every 5 minutes. The data was derived for the entire 2009 year. The distribution of wind speed and direction are represented in Figure 24.

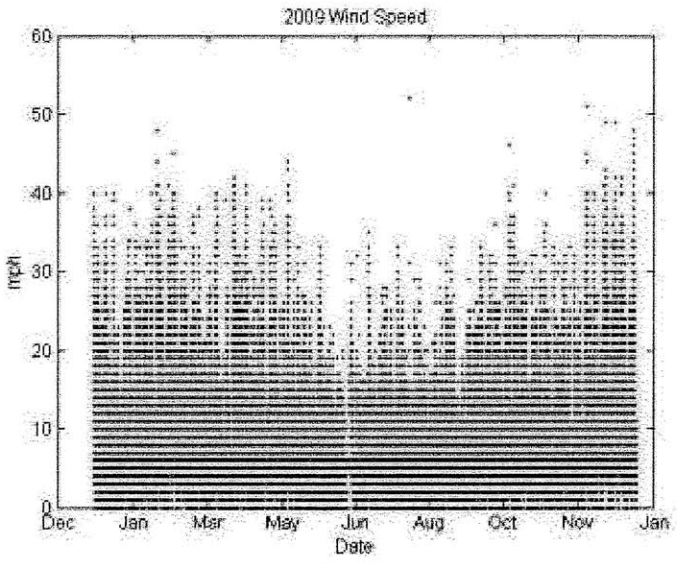

(1) Wind Speed Distribution

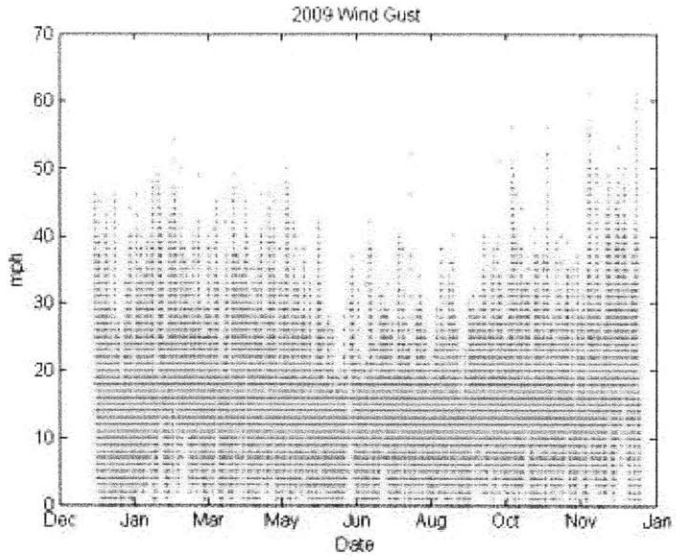

(2) Wind Gust Distribution

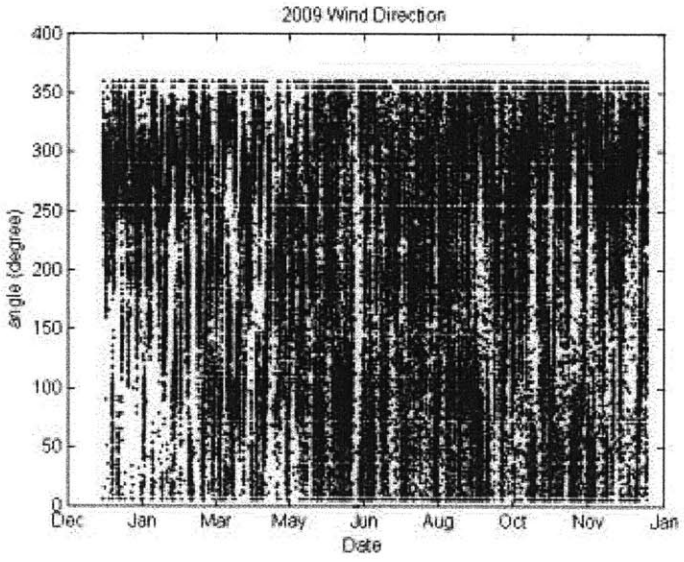

(3) Wind Direction Distribution

Figure 24: Wind Speed and Direction Distribution

Filtered Data

In order to use the scaling factors found from the experimental result section, it is necessary to restrict the angle of attack (the direction of the wind) to be within 0 and 40 degree relative to the building. The wind direction presented in the wind data refers to the absolute direction. The MacGregor building, however, is oriented such that the top of the building makes a 24 degree angle with the western direction (270degree).

Therefore, the angles of interest are from 296 degree to 336 degree. Wind speed distribution and wind direction after the filter process are shown in Figure 25.

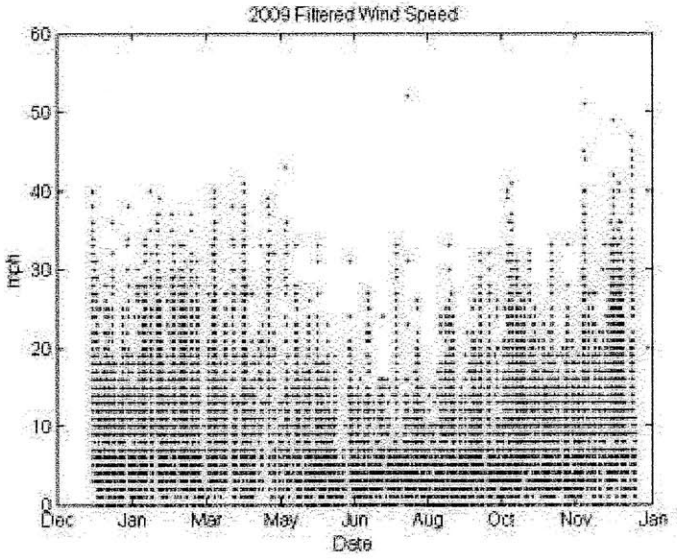

(1) Wind Speed Distribution

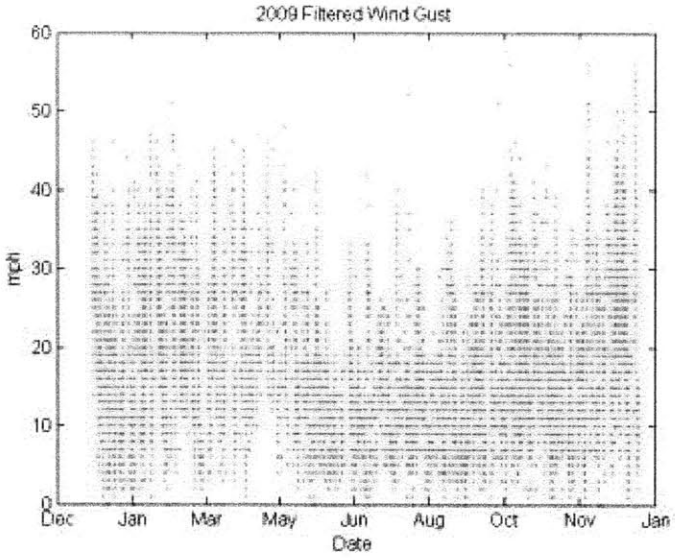

(2) Wind Gust Distribution

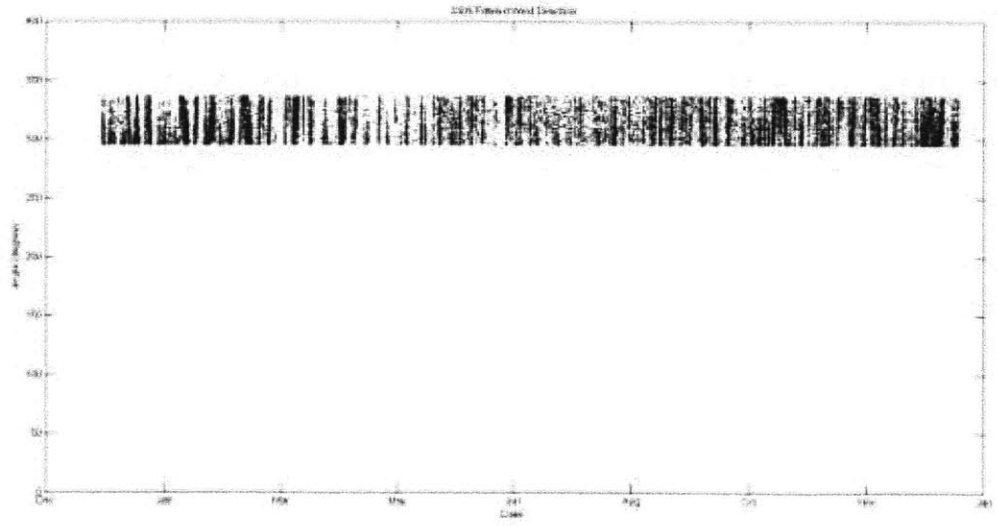

(3) Wind Direction Distribution

Figure 25: Filtered Wind Speed and Direction Distribution

The result of the filter from Figure 25 is quite uniform across the year for the specific angles of interest. It represents 18.43% of all the data sets in the whole year.

Scaling Procedure

A scaling procedure was done by averaging and interpolating the scaling factors for the angle of attacks of 0, 20, and 40 degrees from the result section. Averaging was done across of the scaling factors for all three speeds being testing in the tunnel (20mph, 25mph, 30mph). Interpolating was done using the parabolic fit to the three data points at 0, 20 and 40 degrees to interpolate for the scaling factors for the angles in between. An example of interpolation using quadratic fit is shown in Figure 26 below.

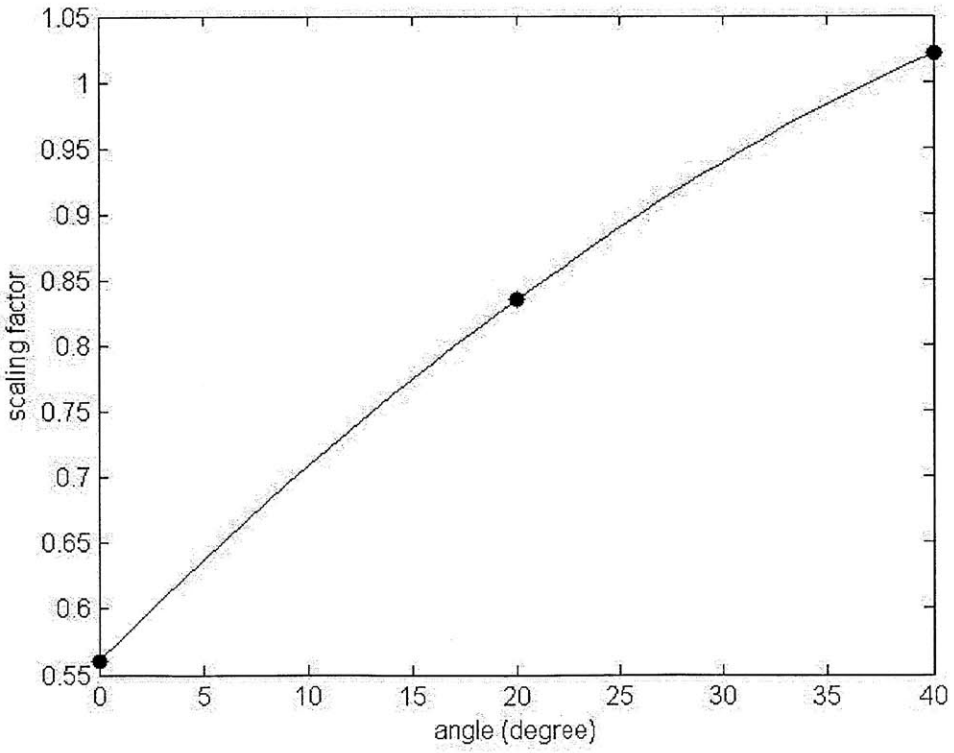

Figure 26: Example of Interpolation for GRID Point 1

Scaling Results

The scaling procedure was done for each different grid point. The results are the predicted wind speed at each grid point for the contact angle between 0 and 40 degrees. Probability density distributions of different wind classes (refer to Table 5) were found using the wind speed of each of the classes as bin edges. The final results are presented as histograms in the following sets of figures:

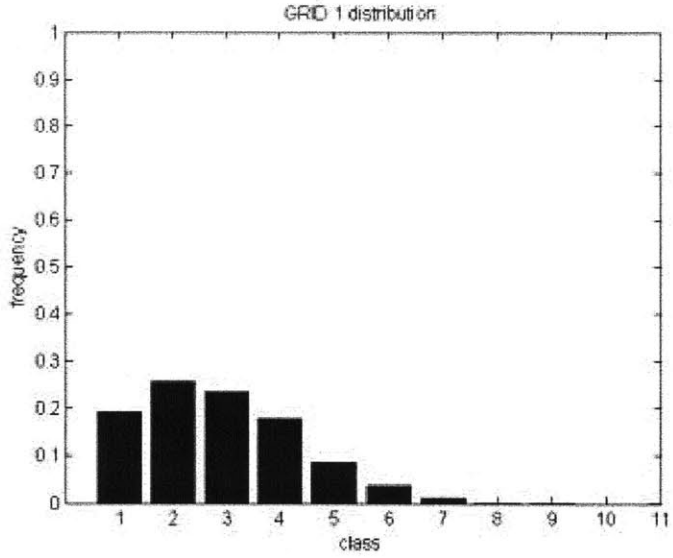

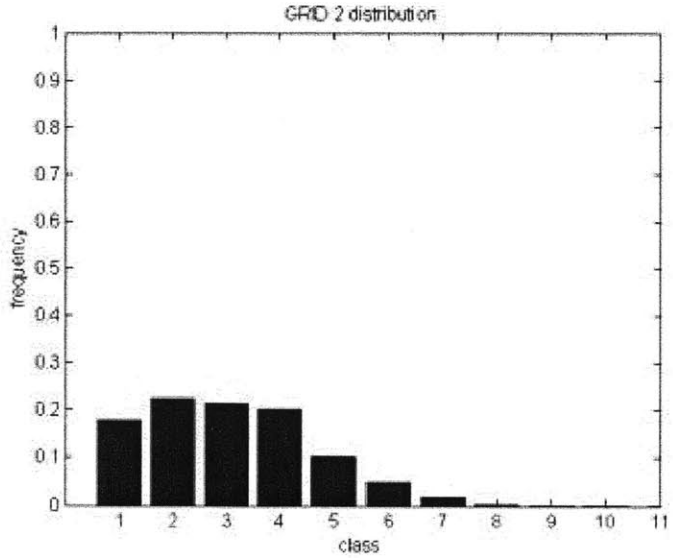

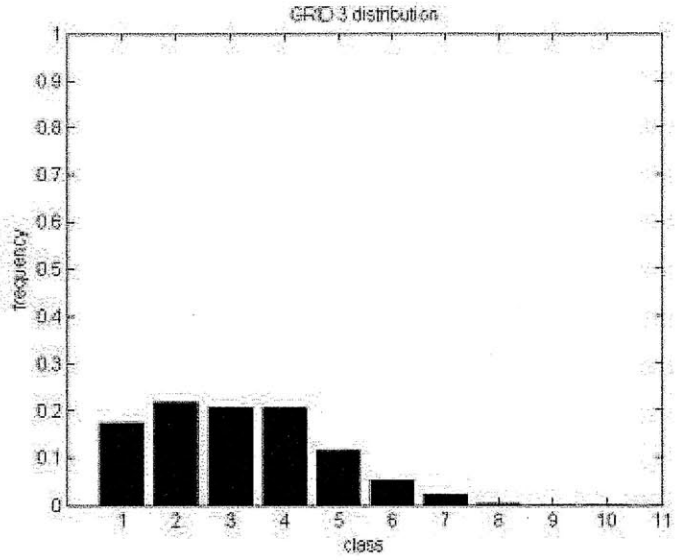
GRID 3 distribution
frequency
class

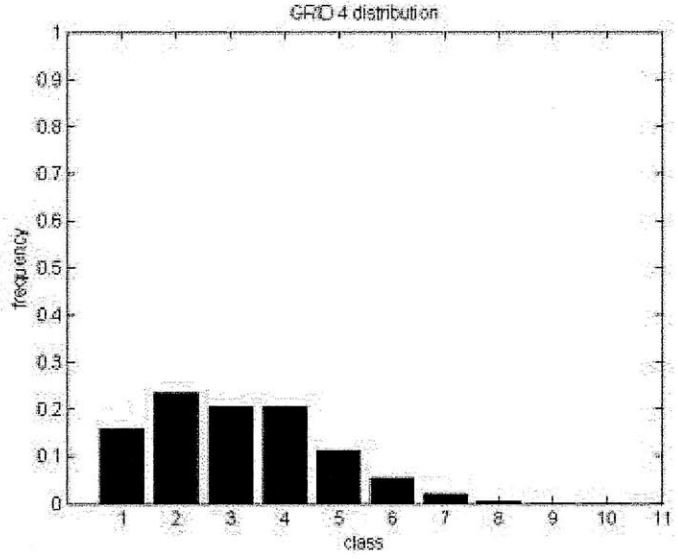
GRID 4 distribution
frequency
class

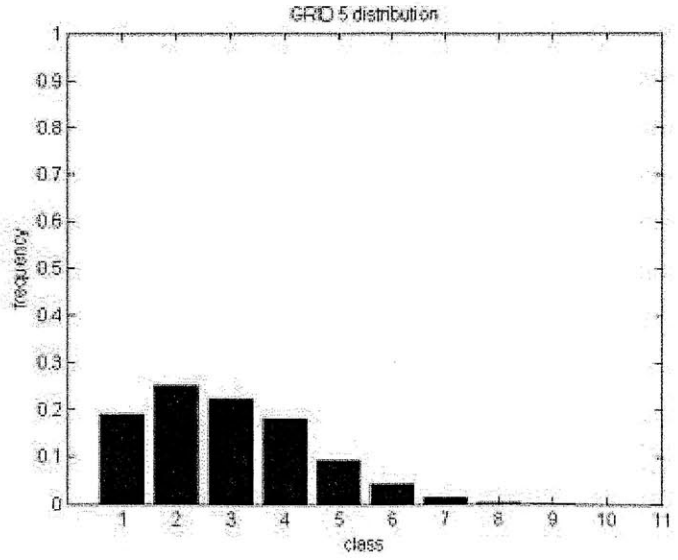
GRID 5 distribution
frequency
class

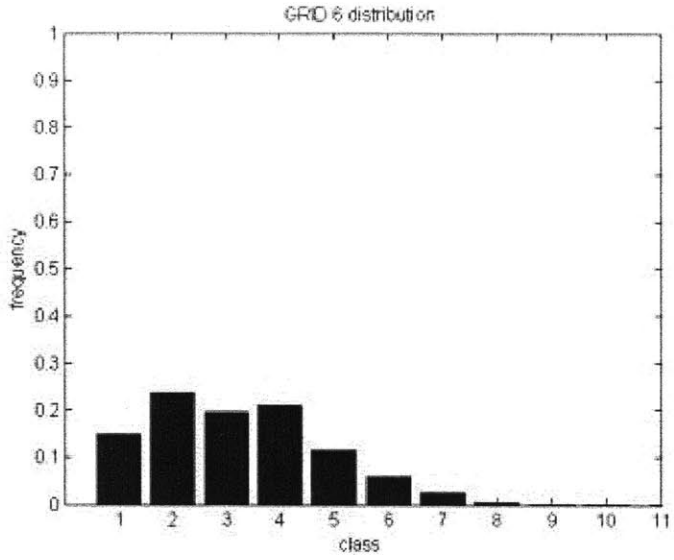
GRID 6 distribution
frequency
class
0
0.1
0.2
0.3
0.4
0.5
0.6
0.7
0.8
0.9
1
1 2 3 4 5 6 7 8 9 10 11

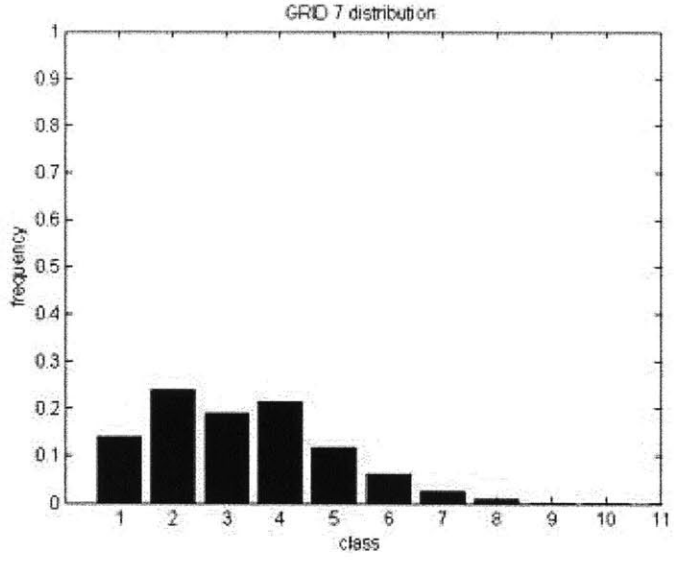
GRID 7 distribution
frequency
class
0
0.1
0.2
0.3
0.4
0.5
0.6
0.7
0.8
0.9
1
1 2 3 4 5 6 7 8 9 10 11

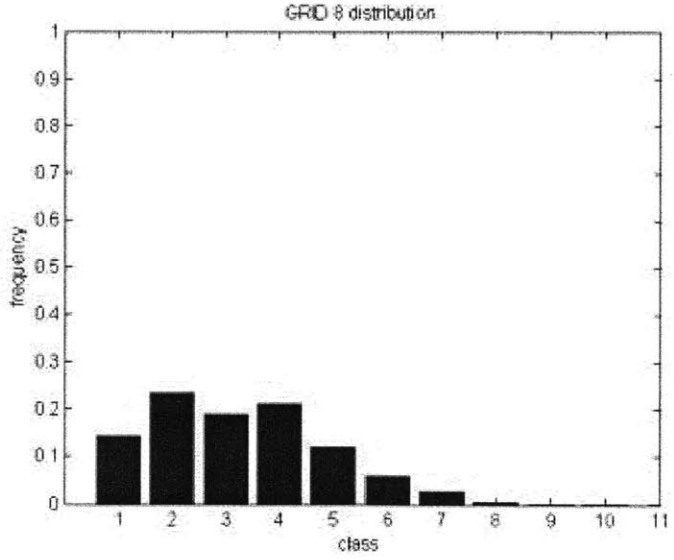
GRID 8 distribution
frequency
class
0
0.1
0.2
0.3
0.4
0.5
0.6
0.7
0.8
0.9
1
1 2 3 4 5 6 7 8 9 10 11

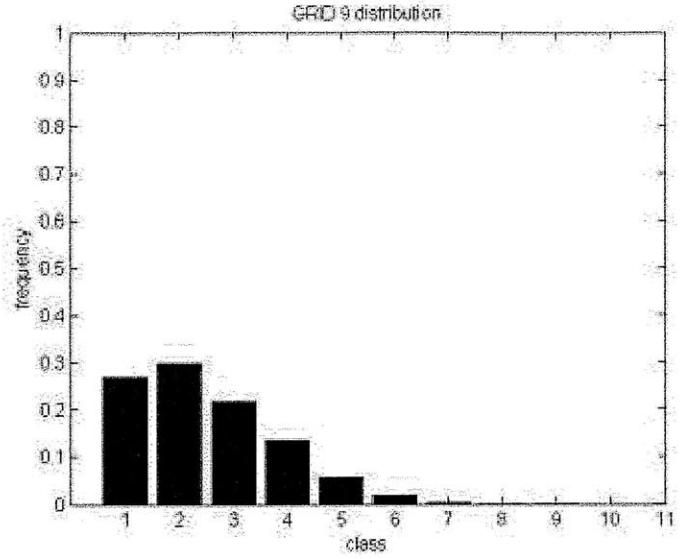
GRID 9 distribution
frequency
class

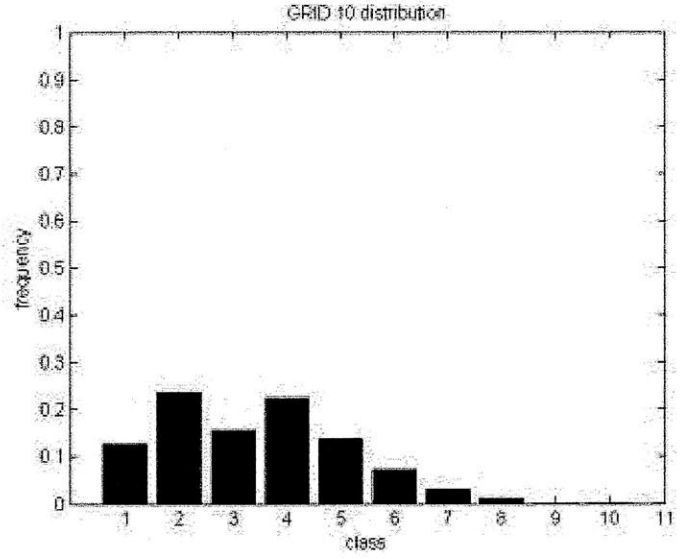
GRID 10 distribution
frequency
class

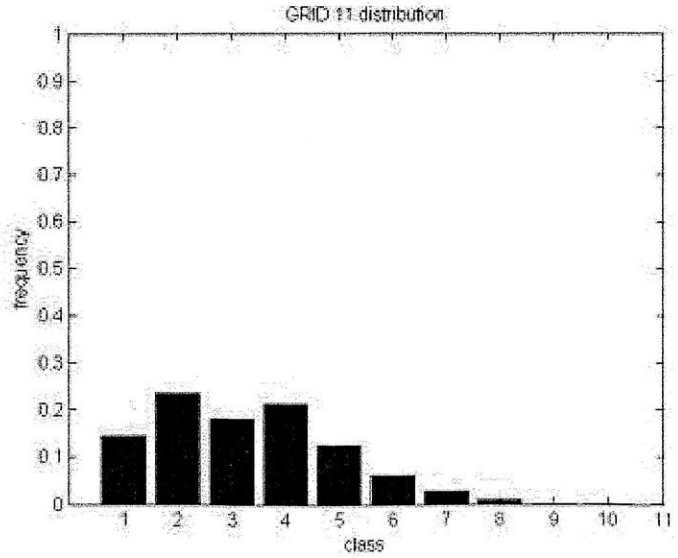
GRID 11 distribution
frequency
class

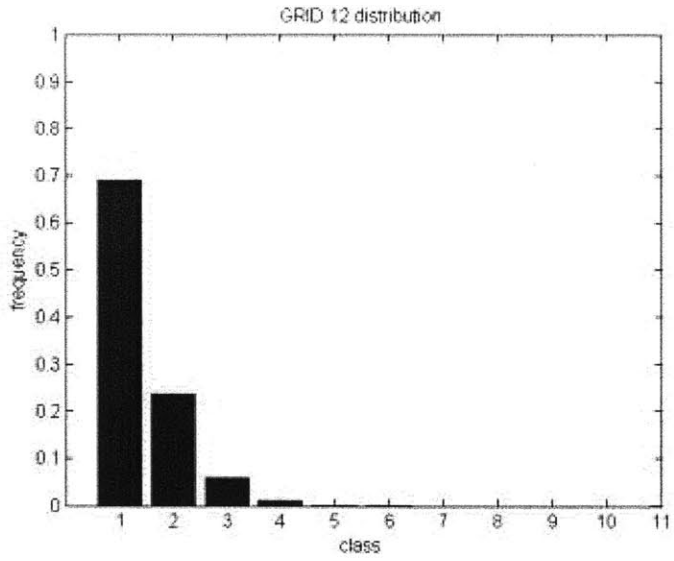
GRID 12 distribution
frequency
class

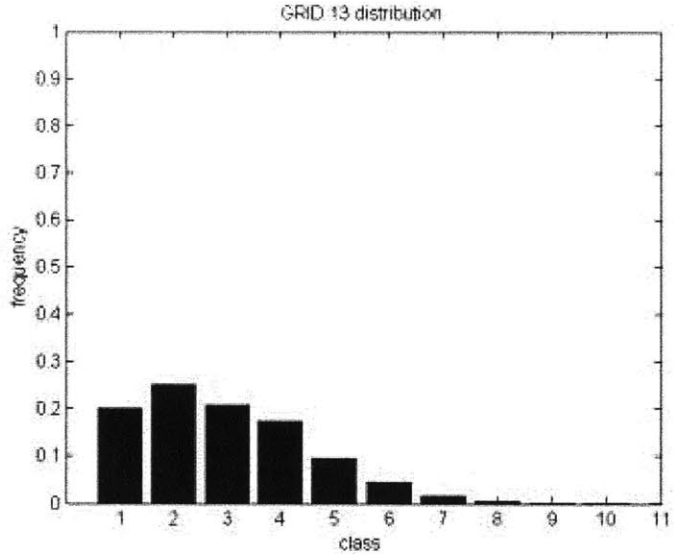
GRID 13 distribution
frequency
class

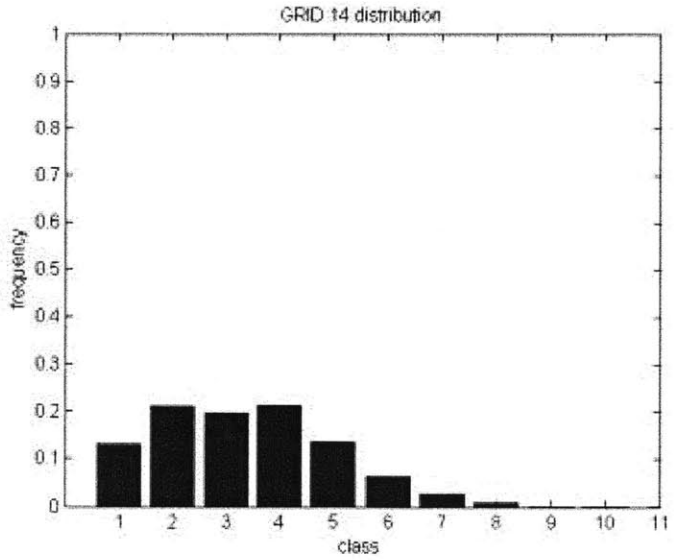
GRID 14 distribution
frequency
class

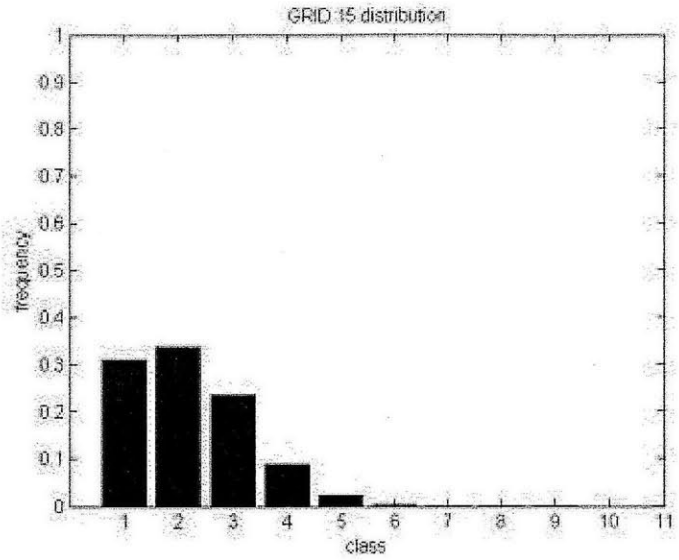

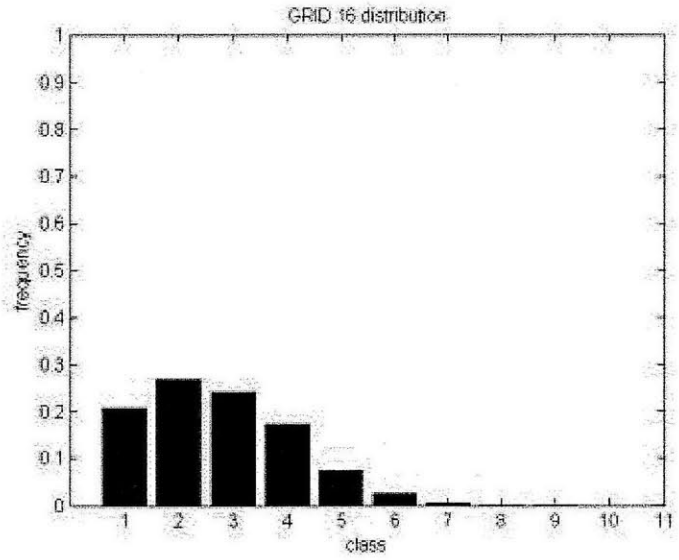

Figures 27-42: Probability Density Distribution of Wind Speed at different GRID Points

GRID	Class1	Class2	Class3	Class4	Class5	Class6	Class7	Class8	Class9	Class10
1	19.46	25.62	23.55	17.82	8.54	3.78	1.03	0.19	0.02	0.00
2	17.96	22.43	21.51	20.23	10.33	5.10	1.94	0.41	0.08	0.01
3	17.47	21.86	20.67	20.48	11.45	5.33	2.19	0.44	0.10	0.01
4	15.96	23.52	20.46	20.56	11.24	5.48	2.16	0.51	0.10	0.01
5	19.14	25.24	22.36	18.03	9.46	4.17	1.31	0.25	0.04	0.00
6	14.97	23.75	19.61	20.99	11.52	5.93	2.59	0.53	0.10	0.02
7	13.94	23.98	18.99	21.56	11.84	6.09	2.65	0.78	0.16	0.02
8	14.54	23.38	19.13	21.39	12.09	6.02	2.77	0.55	0.11	0.02
9	26.83	29.89	21.90	13.46	5.62	1.76	0.43	0.10	0.02	0.00
10	12.67	23.81	15.64	22.51	13.73	7.24	3.02	1.11	0.24	0.04
11	14.54	23.38	18.21	21.27	12.63	6.25	2.72	0.81	0.16	0.03
12	68.93	23.82	5.90	1.16	0.17	0.03	0.00	0.00	0.00	0.00
13	20.19	25.27	20.87	17.32	9.57	4.55	1.54	0.52	0.15	0.03
14	13.35	21.19	19.93	21.59	13.78	6.41	2.73	0.84	0.15	0.03
15	31.09	33.81	23.41	8.86	2.32	0.36	0.12	0.02	0.01	0.00
16	20.70	26.84	24.12	17.43	7.44	2.59	0.68	0.17	0.02	0.00

Table 6: Summary of Probability Density Distribution for each GRID point (as percentage)

Among all the GRIDs, GRIDs 1-8 are the most important as they are on the walkway where most students pass though. Our result actually shows that, for a majority of the time, the wind speed is within an acceptable limit (within or less than class 5). The table below summarizes the probability of wind at each location to be within the limit.

GRID	Class 5 or lower	Beyond Class 5
1	94.98	5.02
2	92.46	7.54
3	91.93	8.07
4	91.74	8.26
5	94.24	5.76
6	90.84	9.16
7	90.32	9.68
8	90.53	9.47
9	97.69	2.31
10	88.35	11.65
11	90.03	9.97
12	99.97	0.03

13	93.21	6.79
14	89.84	10.16
15	99.49	0.51
16	96.53	3.47

Table 7: Summary of Acceptable Wind Speed

We can see that, from the table, there is less than 10 percent of the time at GRID1-8 that the wind is over an acceptable limit. This indicates that the wind problem at MacGregor may not be that particularly serious after all. Among GRID1-8, however, there is an average of 20.13% of the time that the wind is in Class 4, which is described as "raises dust, dry soil, and loose paper." There is also an average of 10.81% that the wind is in Class 5, which described as "force on wind felt on the body." Both of the classes represent a relatively high wind that could be felt on by the pedestrian.

In this regard, Class 4 - inclusive and beyond, together comprises an average of 38.81% among GRID1-8. This represents almost 40% of the time for the condition of our study that the wind could be felt on the body. In particular, since the direction of the wind is in the x-direction, pedestrians are walking directly against the direction where the wind is coming from, and they would certainly feel the effect of the wind. However, we still have to keep in mind that our study is only based on the wind that has the angle of attack relative to the building between 0 and 40 degrees. This representative set comprises 18.43% of the total observations, or 1615 hours out of 8765 hours in the whole year. The strong wind condition (Class 4 and beyond), which is 38.81% of our studies, represents 7.14% of the whole year, or 626 hours total. This number is a significant amount as it represents around 7% of the time that pedestrian will experience high wind conditions. Moreover, this number does not include the wind that is blowing from other directions that could also potentially cause certain high wind conditions.

9. Conclusion

This study has used the wind tunnel model to study pedestrian level wind under the effect of the MacGregor building. Velocity measurement have been done for three different angles of attack (0, 20, and 40 degrees), three different wind speeds (20, 25, and 30mph), and at 16 different grid location around the corner of the building. Smoke measurement has also been performed to observe the wind flow direction.

The results of the velocity measurement were used as scaling factors to predict wind speeds at different grid points across the model. Actual wind speed was obtained from the database for the Green Building at MIT observation station through an online website for the whole 2009 year at a frequency of five minutes per measurement. Scaling factors were used to find predicted wind speeds from the actual wind speed for the wind angles between 0 and 40 degrees relative to the building. The values of scaling factors were interpolated from the values obtained for 0, 20, and 40 degrees.

For angles of attack between 0 and 40 degrees in which we are interested, there is an average of 7.87% that the wind speed is over an acceptable limit among GRID1-8. The density of strong wind speed (Class 4 and above), however, is 38.81% on average. This represents a significant amount of time that the wind is strong around this particular location.

In addition to evidence of strong wind, both from the wind tunnel model testing and from the actual building, the results from the experiment support that there is an accelerated wind condition around the MacGregor building. In the wind tunnel test, the highest measured wind speed is 159% of the far-field wind speed. In fact, many of the wind speeds found in GRID1-8 are above 100% of the far field wind speed.

All in all, the study has analyzed the wind flow around the MacGregor building. It has made predictions, using scaling factors found from the experiment, based on the actual wind data of how strong the wind will be at each particular point around the building. The resulting wind speeds from the prediction seem to fall mostly below the acceptable limit. Further studies, however, will need to verify these findings, and find a way to reduce the wind speed coming from the field in front of the building as this study appears to find little concentration effects (less than 59% accelerated wind condition) as a result of the presence of the building.

10. Acknowledgement

I would like to thank Professor Leslie K. Norford, Richard F. Perdichizzi, Ken Stone of the MIT Hobby Shop, and Surat (Au) Teerapittayanon for their help, suggestions, and contribution to the project. I would also like to thank Brandy Baker, Minshu Zhan, Sharon Xu, Neil Zimmerman, and Alex Kalmikov for providing information related to the project.

11. References

Barenblatt, G. I. Scaling, Self-Similarity, and Intermediate Asymptotics, Cambridge, UK: Cambridge University Press, ISBN 0-521-43522-6. 1996

Bicknell, J., Shaw, A., 'Wind Tunnel Tests of Eastman Court and the Green Building at M.I.T.' Wright Brothers Facility Reports TR 1027-1029, M.I.T. Department of Aero. And Astro., Cambridge, MA, March 1966

Clancy, L. J. Aerodynamics. Pitman Publishing Limited, London, ISBN 0-273-01120-0 Section 3.5, 1975

Durgin, F. H. Proposed Guidelines for Pedestrain Level Wind Studies for Boston – Comparison of Results from 12 Studies. Building and Environment, Vol. 24, No. 4, pp. 305-314, 1989.

Jain, Pramod. Wind Energy Engineering. McGraw-Hill Professional Publishing. ISBN: 9780071714785. September 2010

Kalmikov, Alex et al. Wind power resource assessment in complex urban environments: MIT campus case-study using CFD Analysis. AWEA 2010 WINDPOWER Conference. May 2010.

Penwarden, A.D. Acceptable Wind Speeds in Towns. Build. Sci. Vol. 8, pp. 259-267. Pergamon Press. 1973.

Querin, O.M. Rotor Wake Investigation using the Smoke Flow visualization technique. Univeristy of Sydney. March 1993.

Wannaphahoon, T. A Comparison of the wind speed of MacGregor, New House, and the Massachusetts Bridge. Go Forth and Measure Project. 2009.

Xu, S. Project High Winds: Small-Scale Urban Wind Study. 2011 [the paper is still under revision at the time this thesis is published]

Appendix 1

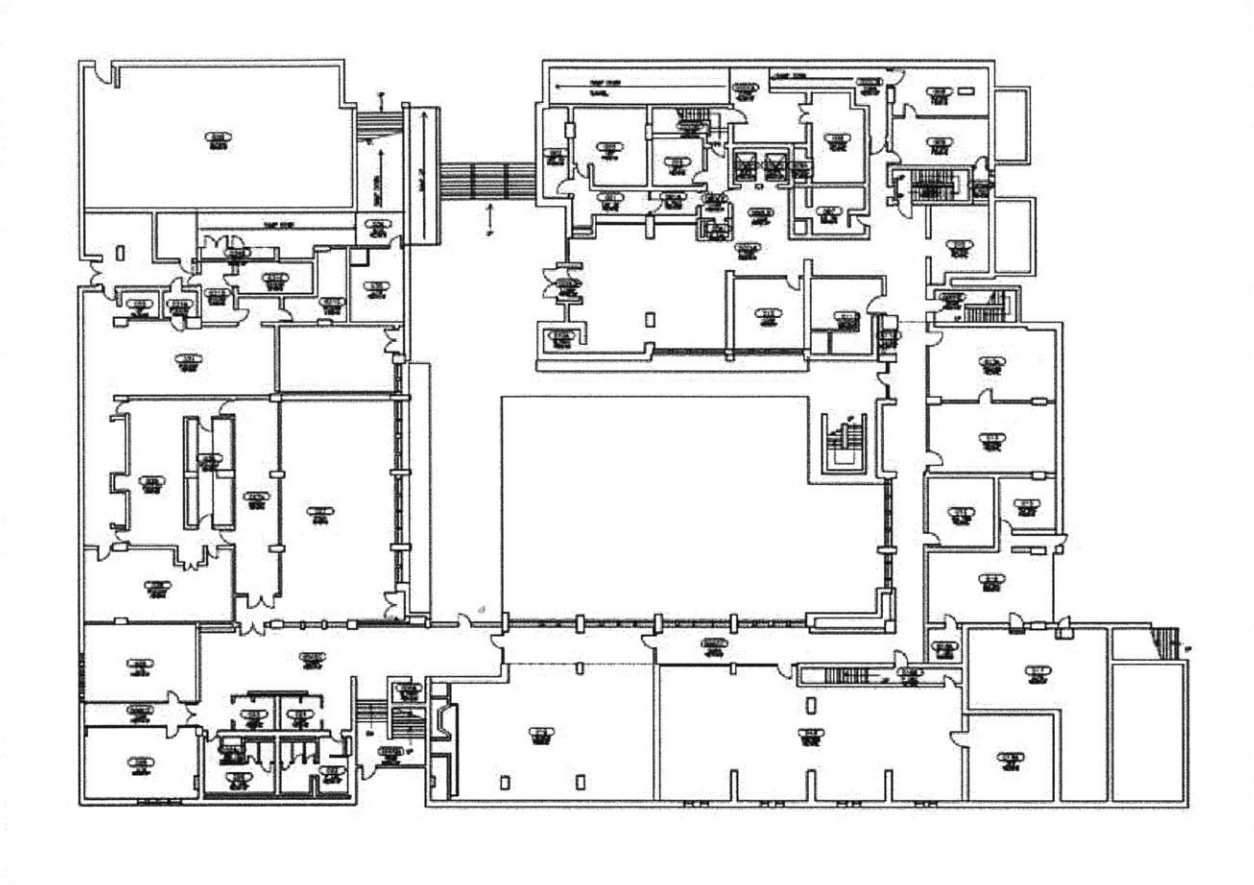

MacGregor floor plan: level 1

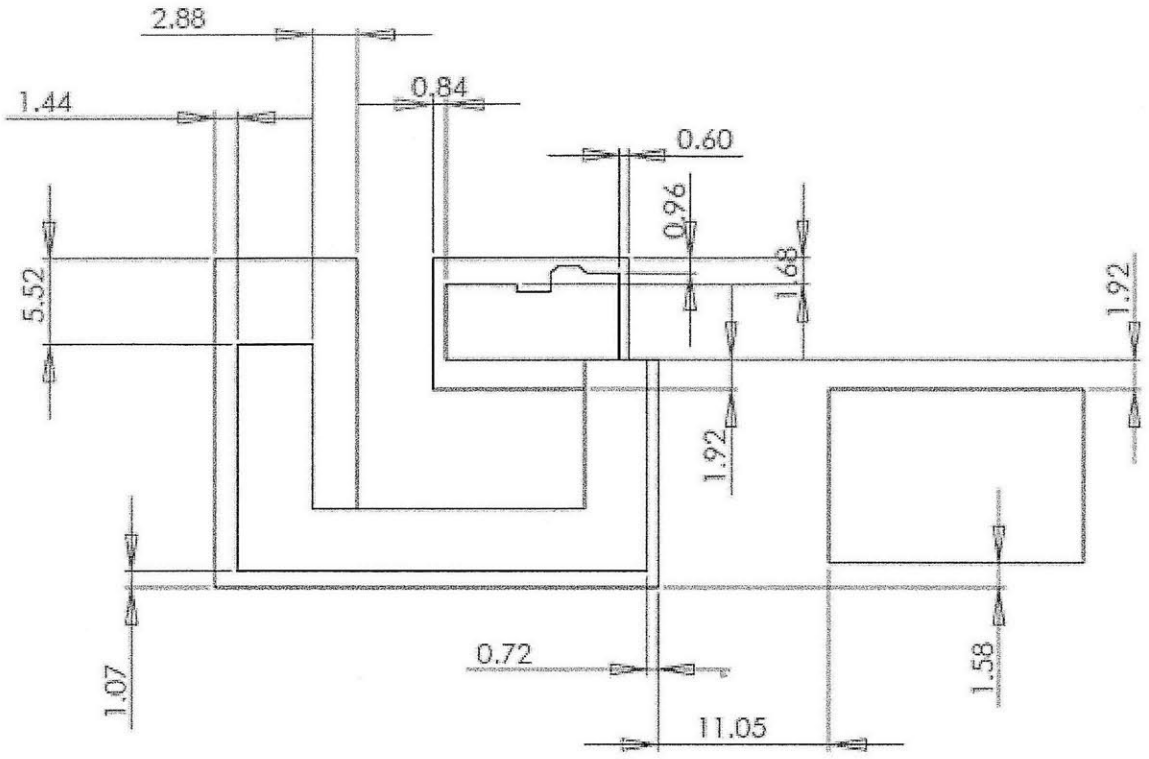

Model in Design (Top)

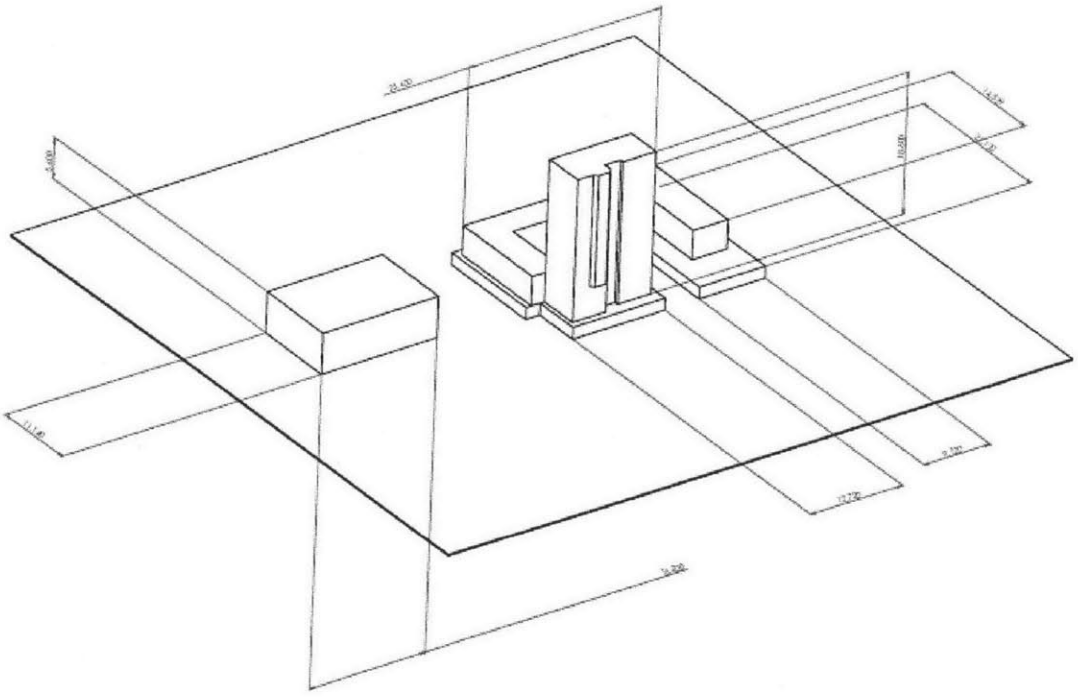

Model in Design (Front)

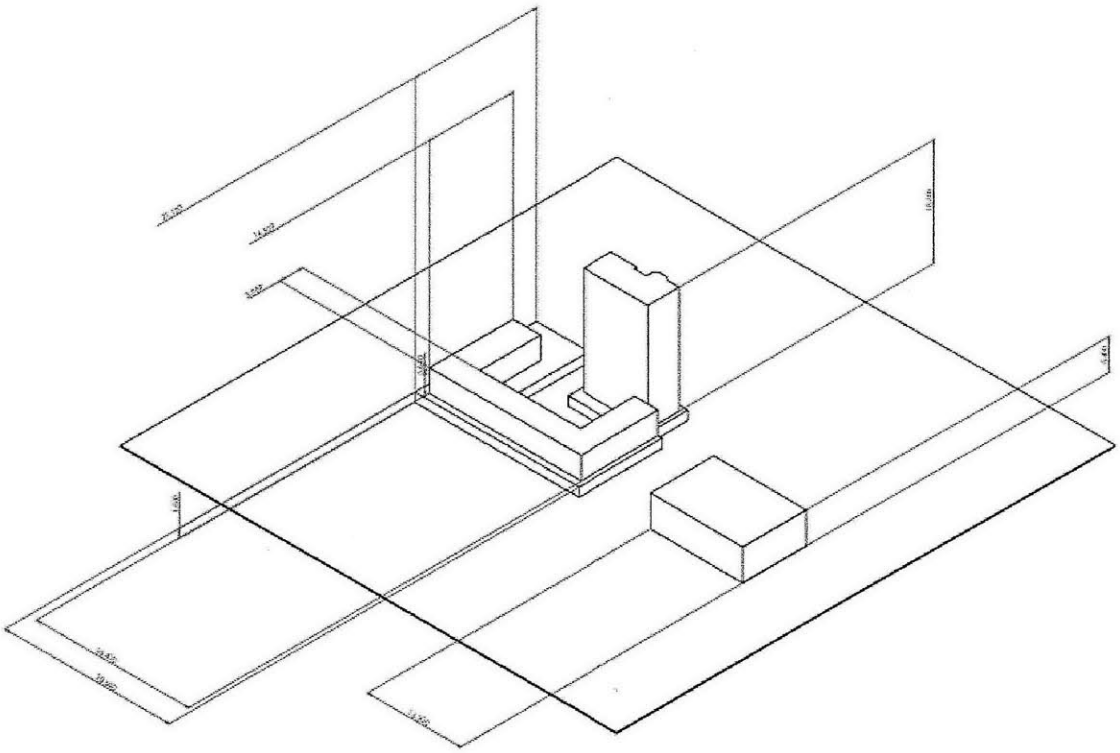

Model in Design (Back)

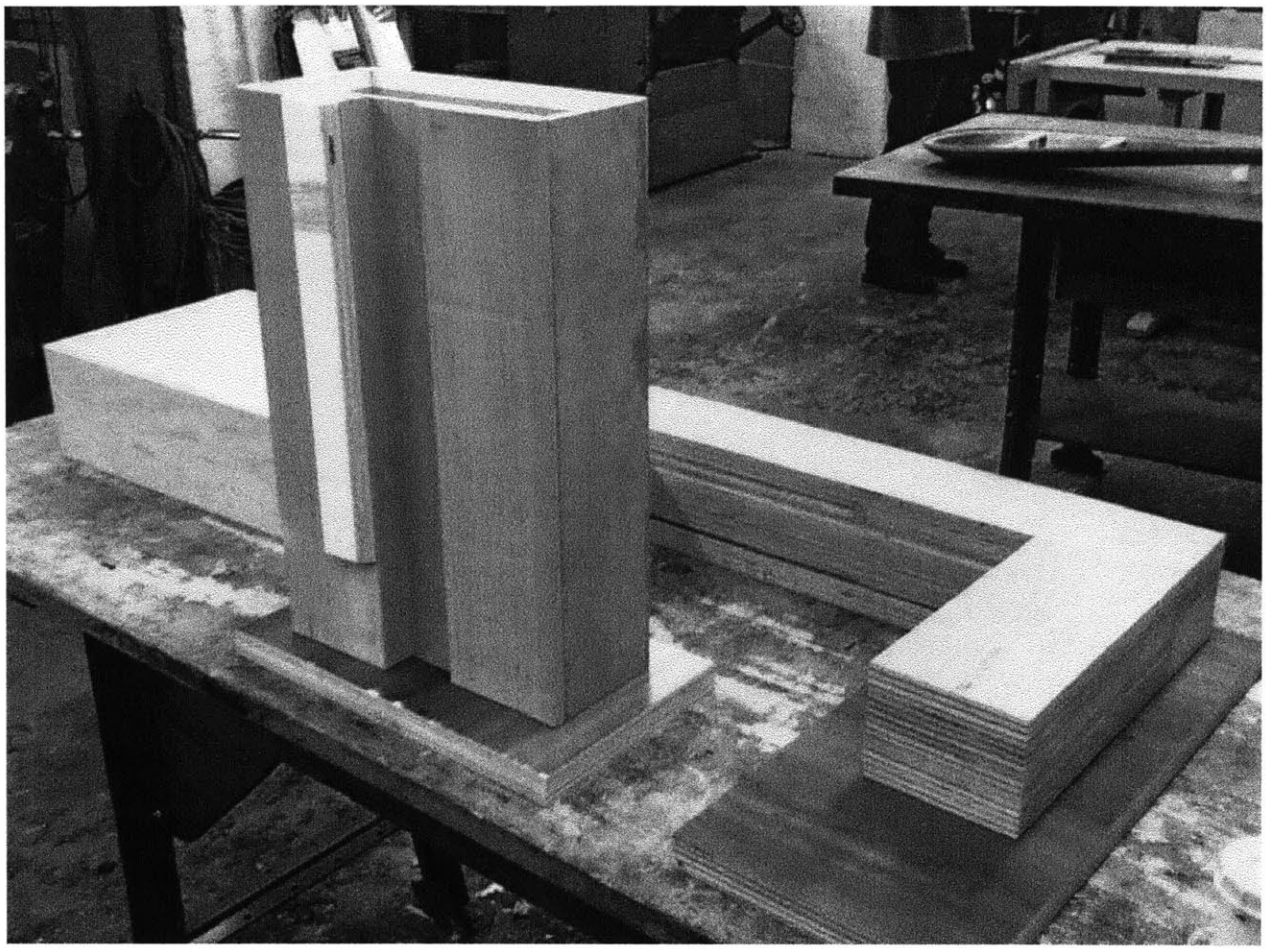

Model before being put on the base

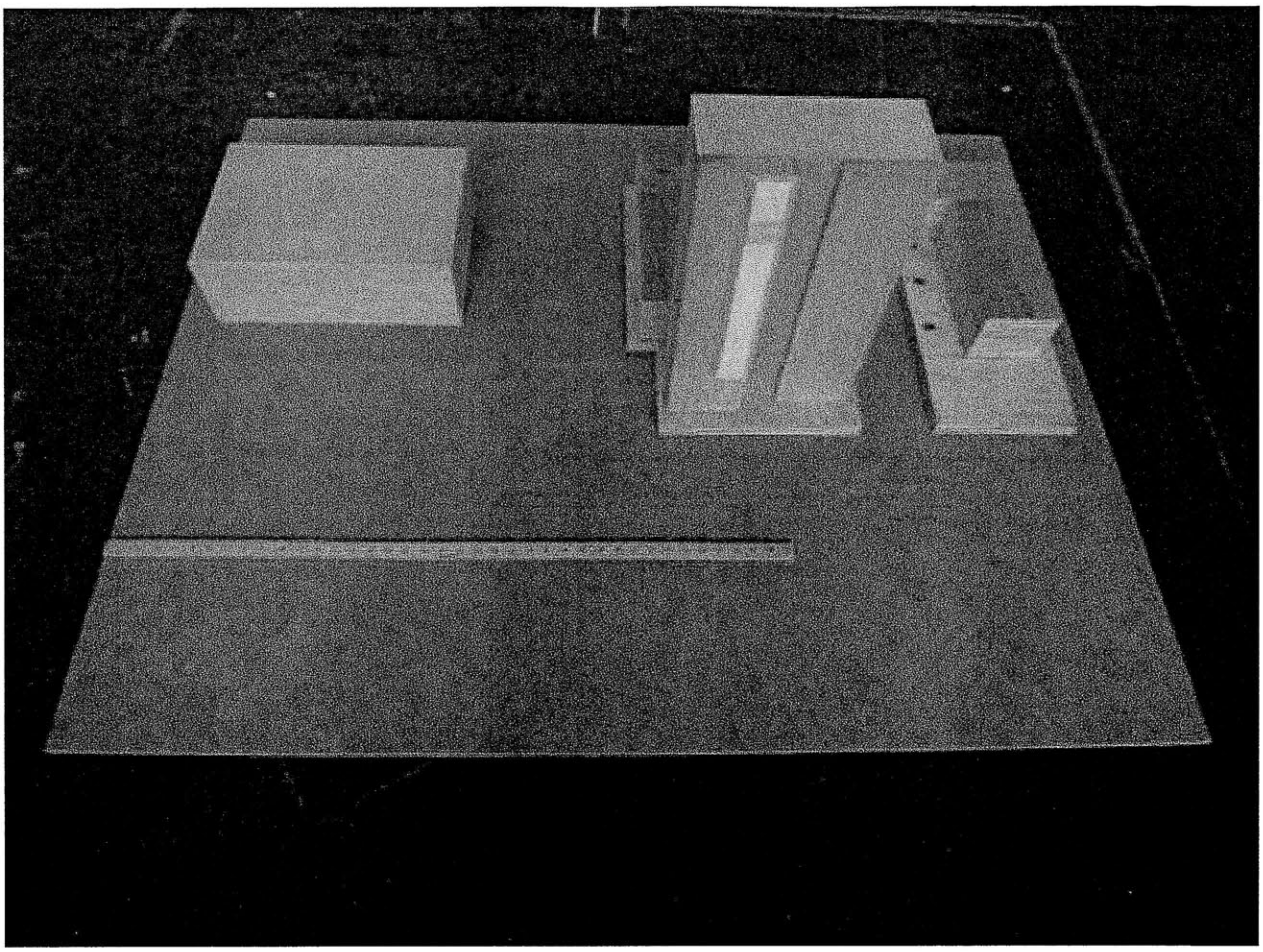

Final Model with the base before the application of black paint to improve the visibility of the smoke and powder used to visualize the airflow.

Appendix 2: Wind Data Resources

Wind Data Results. Unit is in m/s.

Actual Wind Speed 20mph (8.9408 m/s)						
Angle	0	0	20	20	40	40
grid points	Vx	Vy	Vx	Vy	Vx	Vy
1	4.75	2.2	6.25	2.12	9.35	2.12
2	6.5	2.45	8.5	2.71	9.95	2.84
3	6.25	2.95	9.05	2.3	9.9	2.24
4	6.36	4.34	8.9	2.23	10.4	2.16
5	5.4	1.1	8.05	0.95	9.5	2.17
6	7.25	2.5	9.7	1.53	10.2	1.47
7	7.5	2.92	10.16	1.81	10.5	1.86
8	7.7	4.06	9.5	2.09	10.4	2.02
9	9.15	6.2	2.93	4.47	1.6	0.98
10	8.25	3.5	10.8	1.15	10.2	2.75
11	8.1	3.1	10.2	1.35	10.6	1.62
12	2.1	5.45	1.15	2.04	0.87	0.73
13	10	8.9	5.9	6.5	2.5	1.52
14	8.5	5.75	10.9	1.75	8.65	1.75
15	2.6	11.4	2.16	3.96	2	4.61
16	2.25	10.7	2.09	7.85	2.35	2.6

Actual Wind Speed 25mph (11.176m/s)						
Angle	0	0	20	20	40	40
grid points	Vx	Vy	Vx	Vy	Vx	Vy
1	6.6	5.2	10.1	3.5	11.3	2.2
2	7.4	3.85	11.5	2.89	12.1	2.07
3	9	3.38	11.8	2.95	12.3	2.08
4	8.45	5.2	11	2.93	12.7	2.37
5	7.35	1.53	10.5	1.25	11.3	2.4
6	9.5	2.19	12	1.75	12.9	2.9
7	10.1	3.35	12.3	2.25	12.8	2.24
8	10	3.9	12.3	2.42	12.7	2.42
9	11.7	6.85	9.25	6.75	2.62	1.8
10	11.4	5.65	13.2	2.11	13.1	3.2
11	10.5	4.53	11.9	2.05	13.3	1.87
12	3.3	9.45	1.55	2.7	0.93	1
13	12.1	11.7	10.9	11.2	2.41	2.27
14	11	6.35	13	7	10.4	5.45
15	2.06	13.8	2.91	5.65	2.61	8.15
16	4.16	13.3	3.2	11	3.14	4.9

Actual Wind Speed 30mph (13.4112m/s)						
Angle	0	0	20	20	40	40
grid points	Vx	Vy	Vx	Vy	Vx	Vy
1	7.5	6.35	12.1	5.95	13.5	3.5
2	10.7	4.75	13.1	4.4	13.8	3.91
3	11	4.19	13.7	3.84	14.2	3.5
4	10.2	4.69	14.7	4.07	14.2	3.45
5	9.4	1.66	13.1	2.48	13.5	4.04
6	11.8	2.7	15	2.35	14.2	3.42
7	12.6	3.82	15.3	2.98	14.4	2.64
8	12.8	5.25	15.1	3.27	14.7	2.8
9	14.4	13.5	13	6.25	1.8	2.75
10	13.4	8.45	16	2.13	16	7.75
11	13.2	5.8	15	2.51	16.2	6.7
12	4.49	10.46	1.75	3.5	0.95	1.43
13	15.4	14.7	11.8	9.6	2.2	3.6
14	14	11	16.5	5.9	3.4	13
15	4.87	18.2	3.1	5.15	4.43	6.25
16	5.6	17.4	4.05	13.05	3.33	5.25

Appendix 3: Normalized Wind Data Results

Each of the data points is normalized by their respective far field velocity. The normalization values are shown here.

Normalized Wind Speed 20mph (8.9408 m/s)						
Angle	0	0	20	20	40	40
grid points	Vx	Vy	Vx	Vy	Vx	Vy
1	0.53	0.25	0.70	0.24	1.05	0.24
2	0.73	0.27	0.95	0.30	1.11	0.32
3	0.70	0.33	1.01	0.26	1.11	0.25
4	0.71	0.49	1.00	0.25	1.16	0.24
5	0.60	0.12	0.90	0.11	1.06	0.24
6	0.81	0.28	1.08	0.17	1.14	0.16
7	0.84	0.33	1.14	0.20	1.17	0.21
8	0.86	0.45	1.06	0.23	1.16	0.23
9	1.02	0.69	0.33	0.50	0.18	0.11
10	0.92	0.39	1.21	0.13	1.14	0.31
11	0.91	0.35	1.14	0.15	1.19	0.18
12	0.23	0.61	0.13	0.23	0.10	0.08
13	1.12	1.00	0.66	0.73	0.28	0.17
14	0.95	0.64	1.22	0.20	0.97	0.20
15	0.29	1.28	0.24	0.44	0.22	0.52
16	0.25	1.20	0.23	0.88	0.26	0.29

Normalized Wind Speed 25mph (11.176m/s)						
Angle	0	0	20	20	40	40
grid points	Vx	Vy	Vx	Vy	Vx	Vy
1	0.59	0.47	0.90	0.31	1.01	0.20
2	0.66	0.34	1.03	0.26	1.08	0.19
3	0.81	0.30	1.06	0.26	1.10	0.19
4	0.76	0.47	0.98	0.26	1.14	0.21
5	0.66	0.14	0.94	0.11	1.01	0.21
6	0.85	0.20	1.07	0.16	1.15	0.26
7	0.90	0.30	1.10	0.20	1.15	0.20
8	0.89	0.35	1.10	0.22	1.14	0.22
9	1.05	0.61	0.83	0.60	0.23	0.16
10	1.02	0.51	1.18	0.19	1.17	0.29
11	0.94	0.41	1.06	0.18	1.19	0.17
12	0.30	0.85	0.14	0.24	0.08	0.09
13	1.08	1.05	0.98	1.00	0.22	0.20
14	0.98	0.57	1.16	0.63	0.93	0.49
15	0.18	1.23	0.26	0.51	0.23	0.73
16	0.37	1.19	0.29	0.98	0.28	0.44

Normalized Wind Speed 30mph (13.4112m/s)						
Angle	0	0	20	20	40	40
grid points	Vx	Vy	Vx	Vy	Vx	Vy
1	0.56	0.47	0.90	0.44	1.01	0.26
2	0.80	0.35	0.98	0.33	1.03	0.29
3	0.82	0.31	1.02	0.29	1.06	0.26
4	0.76	0.35	1.10	0.30	1.06	0.26
5	0.70	0.12	0.98	0.18	1.01	0.30
6	0.88	0.20	1.12	0.18	1.06	0.26
7	0.94	0.28	1.14	0.22	1.07	0.20
8	0.95	0.39	1.13	0.24	1.10	0.21
9	1.07	1.01	0.97	0.47	0.13	0.21
10	1.00	0.63	1.19	0.16	1.19	0.58
11	0.98	0.43	1.12	0.19	1.21	0.50
12	0.33	0.78	0.13	0.26	0.07	0.11
13	1.15	1.10	0.88	0.72	0.16	0.27
14	1.04	0.82	1.23	0.44	0.25	0.97
15	0.36	1.36	0.23	0.38	0.33	0.47
16	0.42	1.30	0.30	0.97	0.25	0.39